Evidence for late Pleistocene hydrologic and climatic change from Lake Otero, Tularosa Basin, south-central New Mexico

Bruce D. Allen, David W Love, and Robert G. Myers

New Mexico Geology, v. 31, n. 1 pp. 9-25, Print ISSN: 0196-948X, Online ISSN: 2837-6420.
https://doi.org/10.58799/NMG-v31n1.9

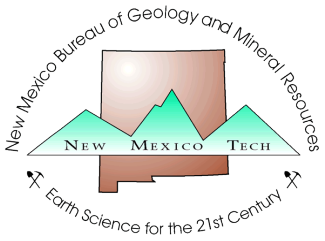

This page is intentionally left blank to maintain order of facing pages.

Evidence for late Pleistocene hydrologic and climatic change from Lake Otero, Tularosa Basin, south-central New Mexico

Bruce D. Allen, New Mexico Bureau of Geology and Mineral Resources, Albuquerque Office, New Mexico Institute of Mining and Technology, 2808 Central Ave. SE, Albuquerque, New Mexico 87106, allenb@gis.nmt.edu; *David W. Love*, New Mexico Bureau of Geology and Mineral Resources, New Mexico Institute of Mining and Technology, 801 Leroy Place, Socorro, New Mexico 87801; *Robert G. Myers*, U.S. Army, IMWE-WSM-PW-E-ES, White Sands Missile Range, New Mexico 88002

Abstract

Stratigraphic relations, lithofacies, and radiocarbon chronology of deposits that accumulated in and around the margins of late Pleistocene Lake Otero in south-central New Mexico provide evidence for the timing and relative magnitude of episodes of lake expansion that occurred in the basin during the last ice age. The lower few meters of stratified sediment in exposures along the margins of the wind-deflated floor of Tularosa Basin contain gypsiferous lithofacies, sedimentary structures, and fossils indicating deposition along the margins of a shallow saline lake. Radiocarbon dates indicate that these basal nearshore lake deposits accumulated from about 45,000–28,000 ^{14}C yrs B.P. A widespread erosional episode removed at least 2 m of lake-margin deposits between 28,000 and 25,000 ^{14}C yrs B.P. Lakebeds overlying the erosional unconformity contain a relative abundance of siliciclastic sediment and aquatic fossil organisms suggesting repeated episodes of increased precipitation, surface runoff, and freshening of the lake system. These inferred episodes of increased precipitation and enhanced fluvial activity in the basin began ca. 24,500 ^{14}C yrs B.P. and lasted for at least 9 millennia. Highstands of the lake during this period appear to have reached an elevation of ~1,204 m. Details of the history of Lake Otero after 15,500 ^{14}C yrs B.P. remain sketchy due to wind deflation of the basin floor and wholesale removal of lacustrine deposits during the Holocene. The evidence from Lake Otero for the onset of maximum pluvial conditions during the late Pleistocene appears to be in good temporal agreement with lacustrine reconstructions from neighboring lake basins to the north and south. Additional study of the deposits associated with Lake Otero, including their abundant and diverse assemblages of aquatic fossil organisms, is clearly warranted.

Introduction

Studies of ancient lake deposits play an important role in documenting late Quaternary climate change (e.g., Bradley 1999; Cohen 2003). In particular, stratigraphic, geomorphic, and chronologic evidence for the growth and demise of perennial lakes and wetlands that lie in hydrologically sensitive arid regions of the world provide relatively direct geological evidence for profound temporal shifts in patterns of moisture transport over the continents. Documentation of the timing and magnitude of these climatic-hydrologic changes at local and regional scales thus provides basic information regarding past changes in Earth's atmospheric-oceanic circulation system. A growing number of researchers are attempting also to quantify rates of biological speciation and other evolutionary trends through the study of populations of aquatic organisms that colonize newly created wetlands or become isolated as wetland areas shrink due to long- and short-term changes in landscapes and climate (e.g., Johnson et al. 1996; Seehausen 2002; Lema and Nevitt 2004; Echelle et al. 2005). Geologic information concerning the timing of wetland expansions and contractions is an obvious complement to such studies.

Unraveling the history of climatic and environmental changes that occurred during the most recent glacial-interglacial cycle has resulted in considerable work in the paleolake basins of western North America (e.g., Smith and Street-Perrott 1983; Benson et al. 1990; Hawley 1993). Many lacustrine archives in the region remain essentially unstudied, however. One such lake was located in the Tularosa Basin of south-central New Mexico (Fig. 1). Tularosa Basin is one of the larger topographic basins in New Mexico and is probably best known for its active field of gypsum sand dunes (White Sands). It has been recognized for more than a century (Herrick 1904) that the basin also contains exposures of Pleistocene lake sediments.

Recent geologic mapping and an investigation of alluvial and spring-related deposits in northern Tularosa Basin have allowed us to conduct a preliminary examination of accumulations of sediment associated with the late Pleistocene lake. Exposures of lacustrine deposits are largely limited to the margins of the lake basin, the basin-center lakebeds having been removed by wind deflation. Nonetheless, the lake-margin sediments that remain provide a valuable record of climatically driven hydrologic changes that occurred in the basin during the last glacial episode. In this paper, we summarize basic observations, preliminary chronology and interpretations of sedimentary deposits associated with Lake Otero, and examine the field evidence for maximum elevations reached by the lake during highstands.

Setting

Tularosa Basin (Fig. 1) is a large (~13,700 km^2) topographic basin, lying to the east of the Rio Grande in south-central New Mexico. It is bordered on the north, east, and west by mountain ranges. The low, structurally and erosionally disjointed topographic divide at the southern end of the basin (elevation ~1,227 m; ~4,025 ft) is underlain by eolian deposits and faulted unconsolidated fluvial deposits of the ancestral Rio Grande, which grade southward into the Hueco Bolson of southwestern Texas. The lower piedmont slopes and floor of Tularosa Basin exist today under an arid climatic regime and support desert scrub and grassland plant communities of the northern Chihuahuan Desert biome.

Surface runoff drains toward the floor of the basin from all sides, but the largest watershed area is on the north side of the basin, reaching elevations as high as 3,649 m (11,972 ft) at Sierra Blanca. (Fig. 1). These northern watersheds sustain permanent wetlands on the floor of the basin today in Salt Creek and at Malpais Spring, both of which support populations of rare, endemic aquatic species, including the White Sands pupfish (*Cyprinodon tularosa* of Miller and Echelle 1975).

Holocene wind deflation of the floor of the basin resulted in the formation of a large (~420 km^2) deflation basin, Alkali Flat (Fig. 2), the floor of which is a playa or ephemeral lake that is essentially devoid of vegetation and is covered by a veneer of mud, sand and gravel washed in during floods, efflorescent salts, and gypsum sand. Lake Lucero is the lowest (elevation ~1,185 m; 3,888 ft) wind-deflated area on Alkali Flat and may contain shallow water for several weeks or more following precipitation events. Many smaller deflation basins and associated eolian landforms are present to the north, east, and south of Alkali Flat (Fig. 2).

As with many of the arid basins in western North America, Tularosa Basin was wetter (Van Devender 1990; Betancourt et al. 2001) and contained perennial lakes during the Pleistocene (Herrick 1904; Meinzer and Hare 1915; Seager et al. 1987; Hawley 1993; Lucas and Hawley 2002). The largest of the late Pleistocene lakes, which formed along the topographically lowest, north-south-trending axis of the basin, was named "Lake Otero" by C. L. Herrick in 1904. Allen (2005) summarized constraints on the size and shape of the lake and the possible existence of many precursor lakes and playas because of the basin's late Neogene geologic history.

Lake Otero deposits

Exposures of sediment associated with Lake Otero are largely restricted to deflation scarps

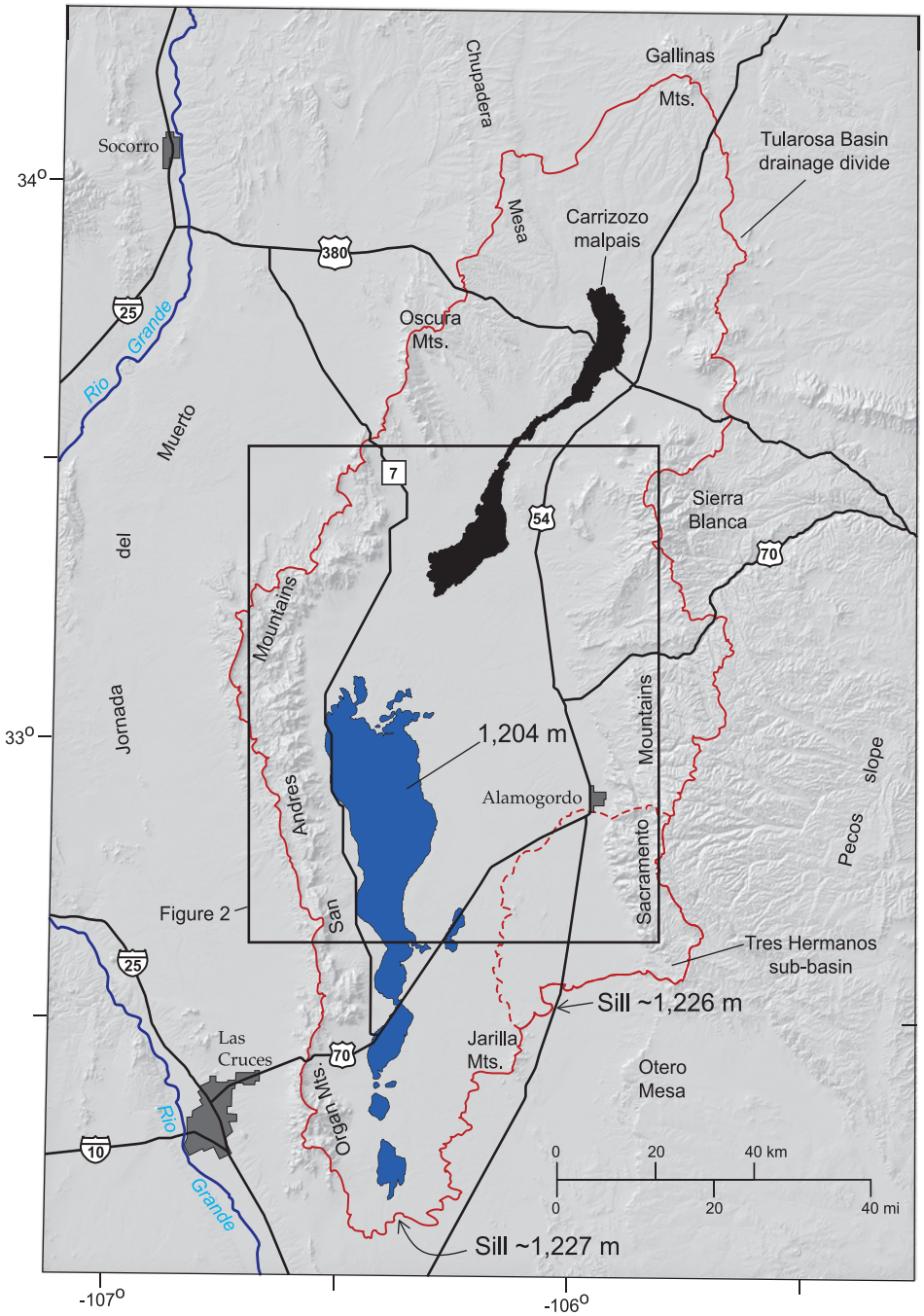

FIGURE 1—Shaded relief map showing the topographic Tularosa Basin (red line) with a surface area of ~13,700 km^2 in relation to surrounding physiographic features, roads, and towns. Area of the basin floor below present-day elevation of 1,204 m (blue fill) corresponds approximately to the extent of Lake Otero during late Pleistocene highstands. Approximate positions of topographic sills (low areas on the drainage divide) at 1,226–1,227 m, and outline of the internally drained Tres Hermanos sub-basin are indicated along the south and southeast margins of the basin. Low point on the Tres Hermanos drainage divide (elevation ~1,217 m) lies approximately 20 km southwest of Alamogordo, just south of US–70. Medial and distal parts of the ~75-km-long, Holocene Carrizozo lava flow (malpais) follow the master drainage for the northernmost part of the basin.

and drainage cuts around the margin of the lake basin. Toward the north end of the lake basin, the deposits associated with Lake Otero become increasingly alluvial in character, reflecting an up-gradient progression from lacustrine to subaerial depositional settings (Lucas and Hawley 2002). More than a 10-m thickness of lake-margin sediment is exposed in deflation scarps along the north edge of Alkali Flat; outcrops of 3–7 m are more typical, and exposures of 2 m or less are commonly encountered in incised drainages.

Herrick (1904) suggested that the exposed sequence of deposits associated with Lake Otero could be divided into lower and upper parts. The basis for this bipartite division was poorly defined and, as noted by Lucas and Hawley (2002), subsequent discussions of the deposits of Lake Otero, beginning with Meinzer and Hare (1915), ignored this distinction.

At some localities along the margins of the lake basin there is indeed a distinct change from comparatively compact, pale-colored, gypsiferous beds near the base of exposures to overlying deposits dominated by siliciclastic mud (Fig. 3). At some localities, the upper and lower lacustrine beds are separated by an erosional unconformity with meters of relief. It is localities such as these that may have led Herrick to propose subdivision of the lacustrine sequence into two formations. In contrast, the sedimentary sequence at other localities, especially along the northern margin of the lake basin where deposits are more alluvial in character, consists of a succession of greenish-gray and reddish-brown muds that are similar in appearance from bottom to top, and the distinction between lower and upper units is not obvious.

Nonetheless, it is meaningful on lithostratigraphic grounds to refer informally to lower and upper parts of the stratigraphic sequence, realizing that all of the outcrops visited during this investigation reflect depositional and erosional processes that acted in proximity to the highstand margins of the lake. In this depositional setting, hiatuses are expected as a result of shallow-water and subaerial erosional processes, as are lithologic variations between correlative deposits at different localities.

Exposures of deposits associated with Lake Otero were examined along the west and north sides of Alkali Flat (Fig. 2). Western-margin sediments were deposited along the front of the San Andres Mountains, which are capped by a thick sequence of Paleozoic carbonate rocks (Kottlowski et al. 1956; Raatz 2002). Northern-margin sediments were deposited at the distal end of a large, low-gradient fluvial system with headwaters extending more than 130 km to the north (Fig. 1). Bedrock units underlying these northern watersheds include thick accumulations of Permian anhydrite (Bachman 1968; Broadhead and Jones 2004), explaining the preponderance of sulfate (gypsum) in the late Pleistocene lake sediments. The deposits of Lake Otero along the western and northern margins of Alkali Flat are discussed separately in the following sections. Similarities and differences exist in the succession of lake-margin deposits between these two areas, which, taken together, provide a reasonably coherent record of the history of the late Pleistocene lake.

Methods

Lake-margin deposits associated with Lake Otero were examined in exposures along the margin of Alkali Flat. Several stratigraphic sections were measured using a Jacob staff and hand level, and samples representing successive lithologic units were collected with a typical sample interval of ~10–20 cm. Descriptions of selected stratigraphic sections are presented in appendices. Interpretations of the individual facies are included in their basic descriptions below.

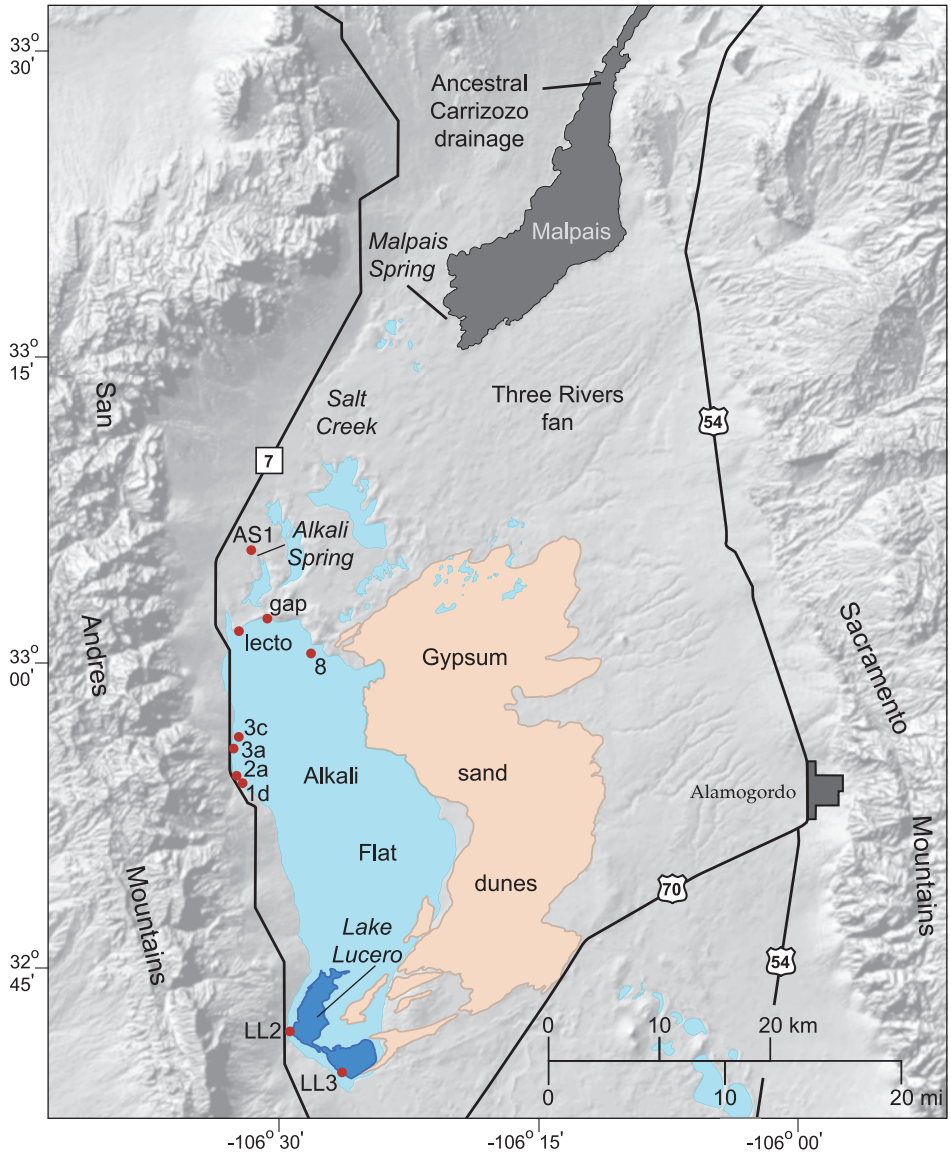

FIGURE 2—Shaded-relief index map of the central Tularosa Basin showing major physiographic features, landforms, and roads. The White Sands dune field (tan fill) covers approximately 600 km^2 downwind from an extensive area of Holocene deflation (deflation basins in pale blue) that removed lakebeds deposited in late Pleistocene Lake Otero. Outline of modern Lake Lucero (lowest area on Alkali Flat) is indicated by dark-blue fill, and the distal end of the Carrizozo lava flow is dark gray. Localities of selected measured sections are labeled red dots.

Representative sediment samples were further characterized in the lab (gypsum, carbonate, and insoluble-residue content) and were dispersed, wet sieved, and the sieve residues examined using a binocular microscope for lithologic components, fossils, and to separate materials for radiocarbon analysis. Separates consisting of ostracode valves, plant fragments, and charcoal were submitted to Beta Analytic, Inc., for radiocarbon age determinations. Gypsum amounts were determined using the technique described by Nelson et al. (1978). Calcium carbonate amounts were determined using a Chittick apparatus (Dreimanis 1962).

Delineation of watersheds and morphometric characteristics including elevations were obtained using geographic information system (GIS) software and 10-m U.S. Geological Survey digital elevation models. Color stereographic 1:24,000 aerial photographs aided in the identification of outcrops and landforms associated with the late Pleistocene lake system.

Western-margin deposits

Lithofacies

Sediments exposed along the western margin of the lake are decimeter- to meter-scale beds of gypsiferous mud, siliciclastic mud, fine-grained gypsum, and interlaminated to thinly interbedded gypsum sand and siliciclastic mud. A few beds 5–15 cm thick are enriched with fine-grained calcium carbonate. The lacustrine sequence along the western margin consists of a lower part containing abundant gypsum (Fig. 4A) and an overlying sequence with an abundance of calcareous, siliciclastic mud (Fig. 5A).

A common lithofacies, particularly in the lower part of the lacustrine sequence, consists of pale-greenish-gray, compact, gypsiferous mud. Gypsum in these beds is evenly dispersed and is present as silt- and sand-sized lenticular grains, commonly twinned, and as larger aggregates of smaller grains. These gypsiferous muds commonly exhibit sub-vertical, decimeter-scale polygonal cracks that appear to be primary sedimentary structures (Fig. 4B). Fossil aquatic organisms are rare. This facies is less common in the upper part of the lacustrine sequence along the western margin.

Fine-grained gypsum beds are generally hard, compact, ledge-forming units. Individual gypsum crystals are predominantly silt-sized, but sand-sized lenticular and hemibipyramidal crystals are present. The gypsum beds are typically structureless in outcrop, but laminated beds are present as well. Some of the laminated beds display polygonal cracks and a distinctive crinkled texture on bedding planes (Fig. 4C), very similar to sedimentary structures formed by algal-mat growth under moist, subaerial conditions seen on modern playas.

Thin beds of dark-brown to black siliciclastic mud (Fig. 4D) containing abundant organic matter, including relatively large (mm-scale) fragments of vascular plants, are interbedded with gypsiferous muds and fine-grained gypsum beds in the lower part of the lacustrine sequence. Fossil ostracodes and mollusks are generally present. Individual black layers appear to be truncated and then reappear laterally on a scale of tens to hundreds of meters, suggesting the presence of local cut-and-fill structures within the lower part of the lacustrine sequence.

Another common lithofacies along the western margin consists of interlaminated to thinly interbedded gypsum sand with varying amounts of siliciclastic mud. Colors range from very pale (gypsum dominant) through shades of brown and greenish gray (Fig. 4E). Individual laminae and beds commonly thicken and thin laterally and are generally discontinuous. In the samples that have been examined, fossil ostracodes and mollusks are rare.

In the lower part of the exposed lacustrine sequence, bedding planes on packages of gypsiferous mud, fine-grained gypsum, and interlaminated gypsum sand and mud exhibit distinctive, subcircular impressions that are interpreted as fossil footprints (underprints) created by large Pleistocene mammals (camels and mammoths; Figs. 4C, 4E; Lucas et al. 2002, 2007; Allen et al. 2006). Some of the depressions are filled with siliciclastic mud; others are filled with coarser-grained gypsum sand. The basal few decimeters of the lacustrine sequence along the south margin of Lake Lucero (east of locality LL3 in Fig. 2) consist of laminated gypsum sand, and contain a remarkable abundance

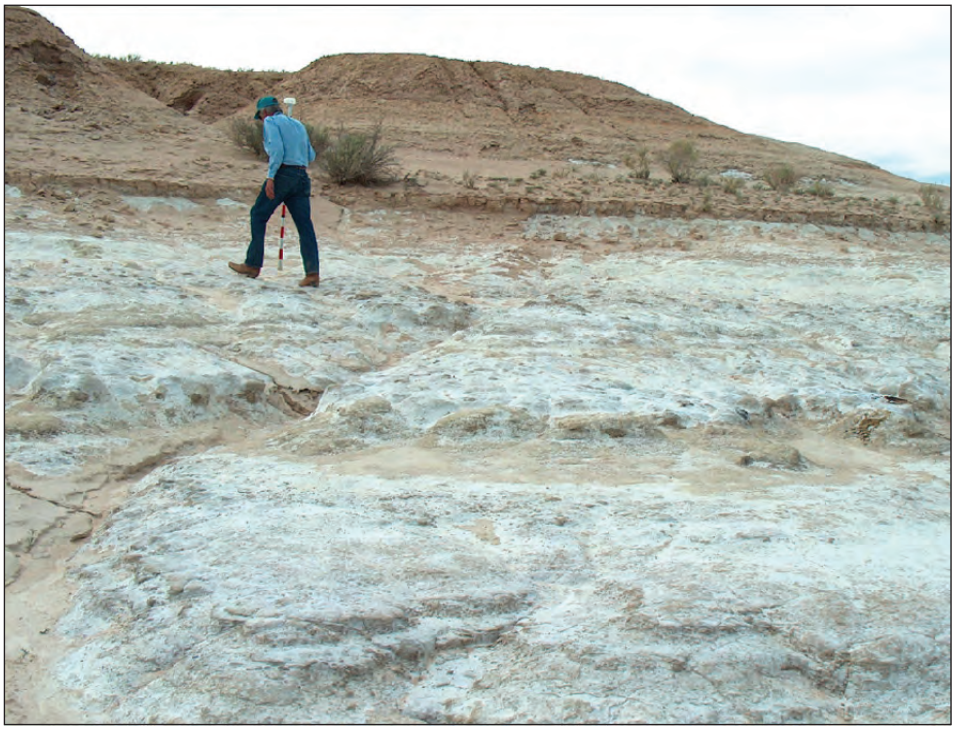

FIGURE 3—Compact, pale-gray gypsum deposits overlain by reddish-brown siliciclastic mud at locality 8 (Fig. 2).

of these fossil tracks. The track disturbances here are filled with recrystallized coarse-grained gypsum.

The upper part of the lacustrine sequence along the western margin contains beds of olive-gray siliciclastic mud with an abundance of fossil ostracodes, gastropods, and vertebrates (fish, amphibians). Coarse, secondary selenite crystals are locally abundant in the siliciclastic beds, disrupting or obliterating primary bedding.

Fine-grained calcium-carbonate muds are also present along the west side of the lake basin. Beds of carbonate mud in the upper part of the lacustrine sequence are generally soft, structureless, and contain fossil ostracodes and aquatic gastropods; sieve residues are dominated by calcareous casts and molds of aquatic plants. The lower part of the stratigraphic sequence along the western margin also contains centimeter- to decimeter-scale beds of calcium carbonate that are indurated and contain vesicular structures resembling tufa (Fig. 4F).

Depositional environments of the western margin

The lower part of the lacustrine sequence in exposures along the western margin of the lake basin consists largely of interbedded gypsum and gypsiferous mud, with lesser amounts of indurated beds of carbonate and thin beds enriched in organic matter. The stratigraphic distribution of lithofacies, sedimentary structures, and fossils in the lower part of the sequence is consistent with deposition along the margin of a saline lake. Gypsiferous muds were probably exposed periodically in a saline mud flat environment, as suggested by abundant intergrowths of lenticular gypsum silt and sand, desiccation cracks, and a paucity of fossil aquatic organisms. Subaerial exposure or shallow water is also indicated by crinkle-laminated gypsum beds suggesting algal-mat growth, and underprints of large land mammals.

Subaqueous deposition is indicated by fine-grained, structureless gypsum beds and layers of black mud containing abundant fragments of aquatic macrophytes, ostracodes, and gastropods. Thin beds of carbonate mud in the lower part of the lacustrine sequence might also indicate subaqueous deposition, although some may have been deposited as tufa in association with subaerial seeps. The lake-margin deposits were episodically subjected to wind deflation or shallow-water erosional processes, as suggested by local features that appear to represent sediment draping and infilling of erosional swales.

Exposures of overlying lake deposits generally extend shoreward (west) from the prominent deflation scarp that defines the west margin of Alkali Flat (Fig. 5A). East of the escarpment, outcrops generally pertain to the lower part of the lacustrine sequence, although in places patches of overlying sediment that have not been removed by deflation are preserved. The contact between the lower and upper part of the lacustrine sequence is an erosional surface with as much as 2–3 m of vertical relief. The succession and thickness of stratigraphic units in the upper part of the lacustrine sequence is rather complicated as it was partly controlled by this erosional topography. In general, however, exposures of the upper part of the lacustrine sequence commonly consist of (1) as much as 2 m or more of olive-gray siliciclastic mud and interbedded, soft carbonate mud (Fig. 5A), and (2) intervals of thinly interbedded to interlaminated siliciclastic mud and gypsum sand (Fig. 5B).

The calcareous muds in the upper part of the lacustrine sequence are commonly mottled with iron- and manganese-oxide stains, and locally contain secondary gypsum as selenite crystals, which impart a massive, churned appearance to the deposits. Fossil ostracodes, mollusks, and, in some beds, foraminifera are abundant, as are carbonate casts and molds of aquatic macrophytes and skeletal elements and scales of fish. Remains of aquatic pulmonate gastropods are especially abundant in interbeds of carbonate mud. A greater abundance and diversity of aquatic organisms in these siliciclastic and carbonate muds, relative to underlying deposits, together with a relative increase in the content of siliciclastics suggest episodes of enhanced precipitation and runoff of relatively fresh, sediment-laden water into the lake.

The calcareous muds in the upper lake-margin sequence can be traced shoreward in drainage cuts to an elevation of approximately 1,204 m (3,950 ft), where they interfinger with alluvial deposits (Fig. 6). Shoreward exposures contain land snails (Gordon et al. 2002) and terrestrial vertebrate remains (Morgan and Lucas 2005), and to the west of Lake Lucero (near locality LL2 in Fig. 2) probable correlative deposits just below an elevation of 1,204 m contain beds of coarse siliciclastic sand, also suggesting proximity to the shoreline of the lake.

Intervals of interlaminated gypsum sand and siliciclastic mud in the upper part of the lacustrine sequence (Fig. 5B) contain little evidence for aquatic organisms, although thin, dark-colored muds enriched in plant fragments are locally present. The laminated, gypsiferous beds in the upper part of the lacustrine sequence are interpreted as representing episodes of lake drawdown and drier climatic conditions relative to those that existed during deposition of beds of fossiliferous, calcareous mud. At some localities beds of gypsiferous mud with desiccation cracks are preserved in the upper part of the lacustrine sequence, suggesting episodes of subaerial exposure of the lake margin.

The upper part of the lacustrine sequence along the western margin is commonly capped by as much as 2 m or more of gypsum sand, with lesser thin interbeds of siliciclastic mud, stringers of carbonate, and fine-grained, compact gypsum (Fig. 5B). The depositional environment of this unit is uncertain. Samples that have been examined do not contain fossils, and the unit is generally poorly exposed, with a thick, weathered covering of gypsum crust. Field relations suggest that this unit was deposited on an erosional surface, as it is found in basinward exposures resting directly on beds of the lower part of the lacustrine sequence. The unit itself has been extensively eroded by Holocene piedmont alluvial processes, and is generally preserved in isolated hummocks.

A generalized sketch of the distribution of depositional units along the western margin of the lake basin is shown in Figure 7.

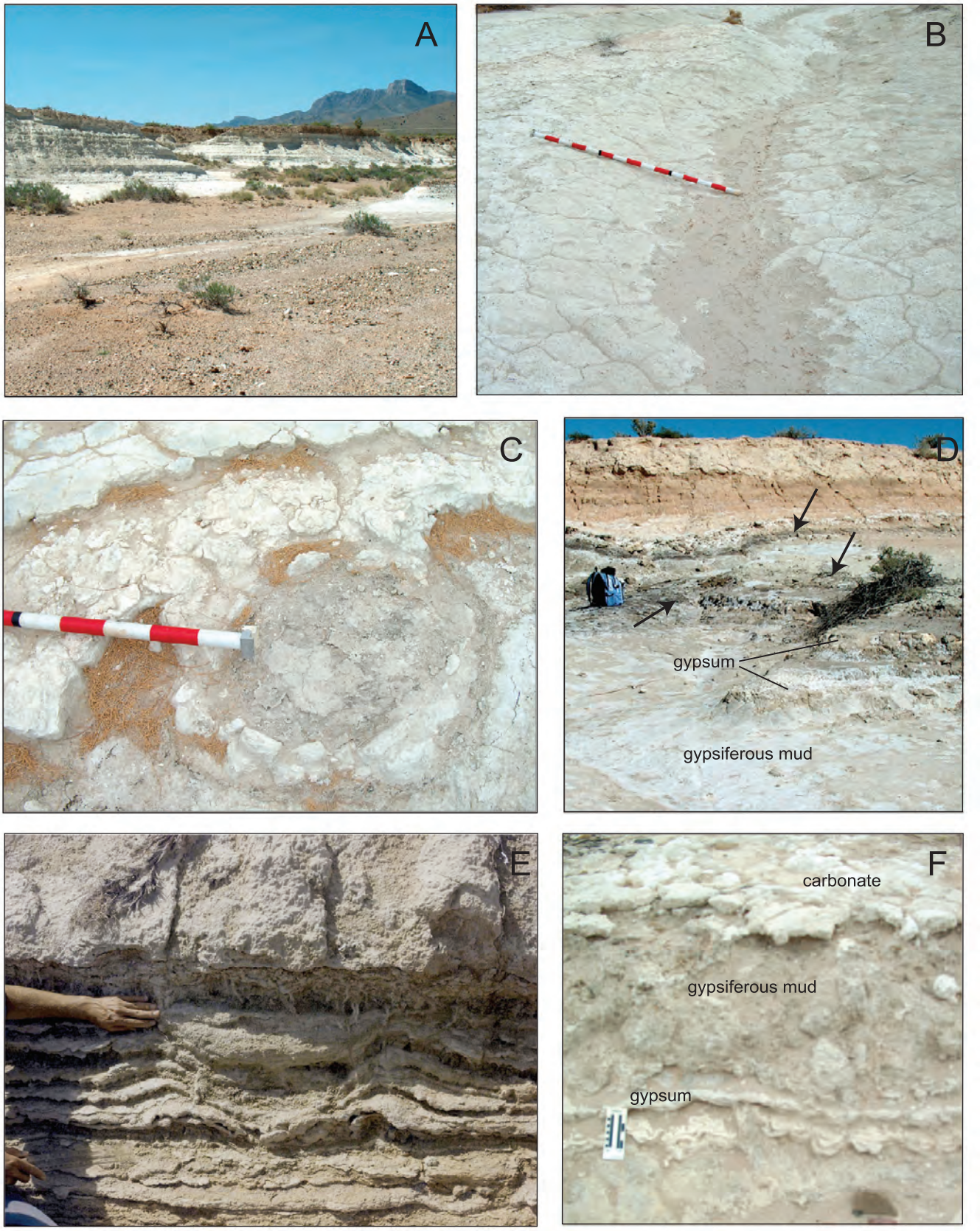

FIGURE 4—Exposures of lower lake-margin facies along western margin of Alkali Flat. **A**—Outcrop showing the planar bedding and pale-gray color characteristic of these gypsiferous deposits. Approximately 3.5 m of lakebeds (capped by Holocene alluvium) are exposed at this locality. **B**—Compact gypsiferous mud facies with polygonal desiccation cracks (rod is 1.5 m long). **C**—Layered gypsum with desiccation cracks (upper layer) and underlying crinkle-folded layer (probably algal structures) disturbed by a proboscidian track (red and white bars are 10 cm long). **D**—Dark layers, rich in organic matter (arrows), interbedded with fine-grained gypsum and compact gypsiferous mud facies at locality 3c. Upper dark layer is draped into an erosional swale in underlying sediments. The lake-margin deposits are overlain by reddish Holocene alluvium and eolian deposits. **E**—Cross section of proboscidian track (underprint) deforming underlying thinly interbedded gypsum sand and siliciclastic mud facies. Track is filled with saucer-shaped plug of gypsum sand. **F**—Thin bed of resistant, tufa-like calcium carbonate on top of gypsiferous muds containing a bed of laminated gypsum with algal structures.

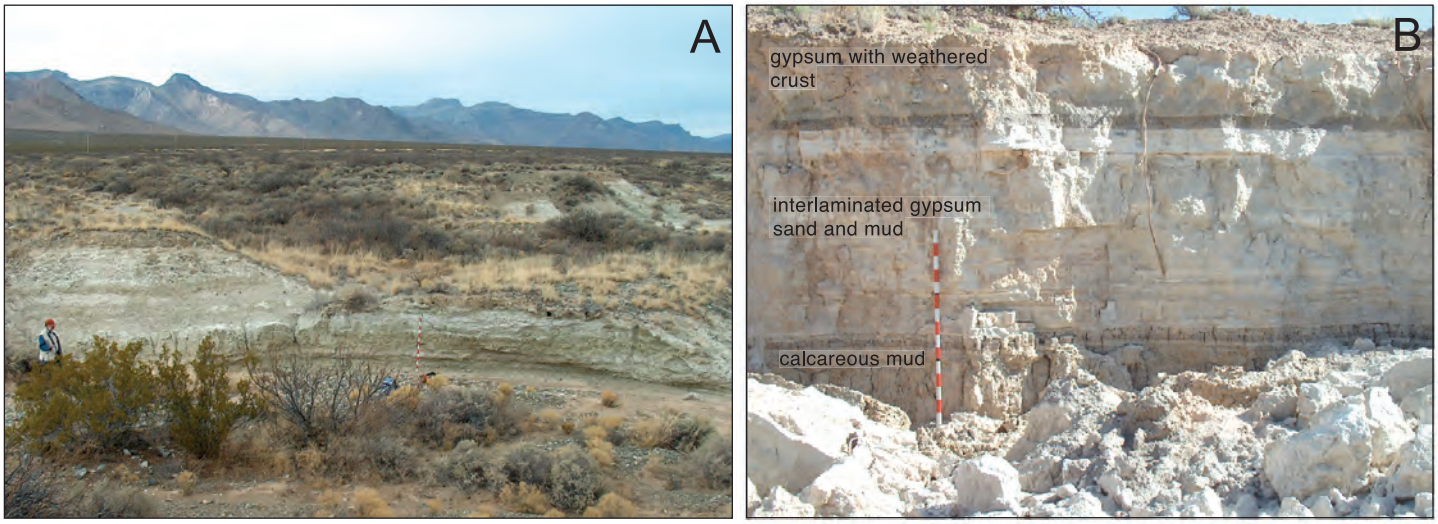

FIGURE 5—Exposures of upper lake-margin facies along western margin of Alkali Flat. **A**—View northwest at deflation scarp and exposure of olive-gray siliciclastic and interbedded calcareous mud extending west under Holocene alluvium. **B**—Drainage cut farther to the west showing sequence of calcareous mud overlain by thinly interbedded gypsum and siliciclastic mud, overlain in turn by gypsum sand with a thick weathered crust (depositional environment uncertain). Locality is near 1d in Figure 2.

Exposures of the lower part of the lacustrine sequence appear to extend to an elevation of approximately 1,198 m (3,930 ft), corresponding roughly to the maximum extent of the lake during accumulation of these sediments. As noted above, deposits pertaining to the upper part of the lacustrine sequence are exposed in drainage cuts to an elevation of 1,204 m. The floor of Lake Lucero (Fig. 2), which is the topographically lowest, wind-deflated area on the floor of the basin today, is at approximately 1,185 m (3,887 ft). Taking into consideration progressive infilling of the lake with sediment during the late Pleistocene, these figures suggest that Lake Otero may have contained, at its deepest, 10–15 m (33–49 ft) of water during highstands.

Post-Lake Otero features along the western margin

Wind deflation and periodic flooding of the basin floor after desiccation of Lake Otero created a series of north-south-trending benches and escarpments along the western side of the lake basin that Langford (2003) refers to as shorelines. These erosional landforms probably reflect progressive wind-excavation of the basin floor, interrupted by periods of comparatively wetter climate and temporary stabilization of the basin-floor (playa) surface. Along the western margin of Alkali Flat, tufa deposits are commonly present on the highest of the erosional terraces at an elevation of approximately 1,198 m (Fig. 8), and less commonly on lower surfaces. The tufa typically consists of a dense meshwork of fibrous calcium carbonate, suggesting a biotic influence during carbonate precipitation. A sample collected from one locality revealed abundant fossil ostracode shells, indicating subaqueous deposition at some localities. The tufa deposits along the western margin suggest an episode (or episodes) of wetter climate and ground water discharge that interrupted the progressive excavation of the basin floor by the wind.

Another notable feature along the western margin is the development of accumulations of large selenite crystals that have grown displacively within the lake-margin

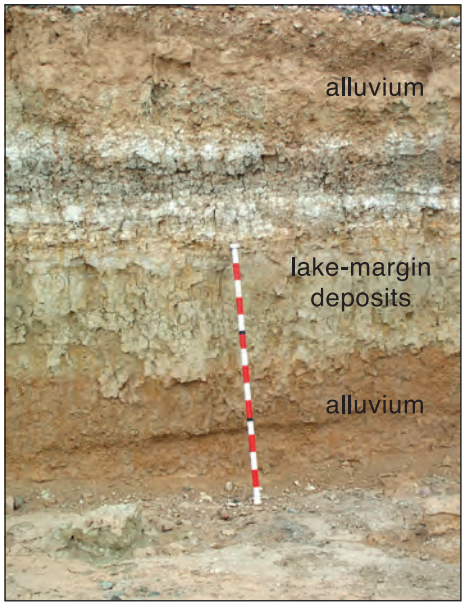

FIGURE 6—Exposure of western-margin deposits at an elevation of ~1,200 m, showing interfingering of lake-margin deposits and piedmont alluvium. Locality is west of 2a in Figure 2.

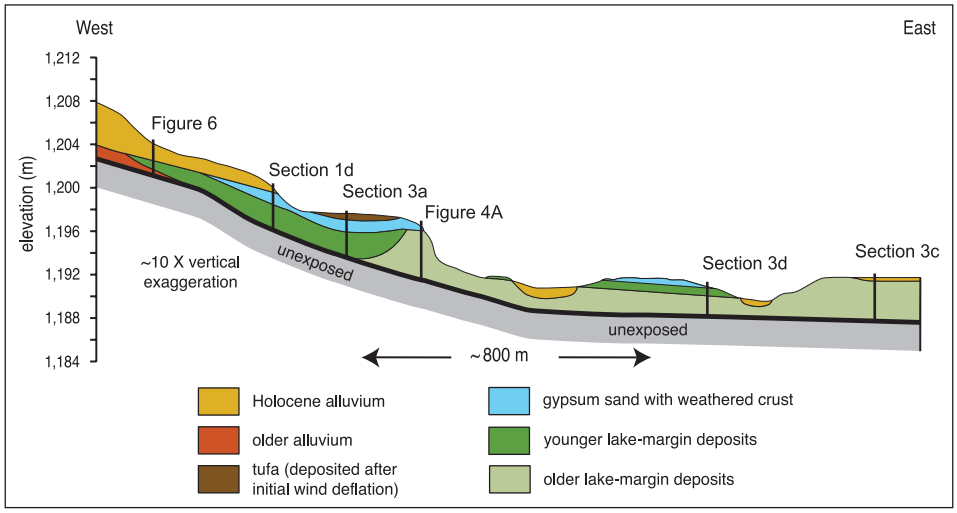

FIGURE 7—Schematic cross section showing distribution of late Pleistocene–Holocene depositional units along the western margin of Alkali Flat. Younger lake-margin deposits (dark-green fill) unconformably overlie and are inset against older lake deposits (pale-green fill), and interfinger with contemporaneous alluvial deposits (orange fill) below 1,204 m. The younger lakebeds are in turn overlain by as much as 2 m or more of gypsum sand with minor siliciclastic mud and carbonate (blue fill). Holocene deflation and subsequent entrenchment of alluvial fans and basinward transport of alluvium has left coarse-grained piedmont deposits (yellow fill) at all levels on the eroded, relict, lake-margin landscape. Approximate positions of selected stratigraphic sections are shown.

FIGURE 8—Post-Lake Otero tufa deposits along west side of Alkali Flat at 1,198-m elevation (near locality 3a in Fig. 2). Scale in centimeters.

FIGURE 9—Large amber-colored selenite crystals in greenish-gray, lake-margin siliciclastic mud along west side of Alkali Flat (east of locality LL2 in Fig. 2). The discoidal crystal habit of these large crystals is similar to crystals grown in a clay medium from concentrated solutions containing small amounts of organic acids (Cody 1991; Cody and Cody 1988). Individual tabular fragments are the result of a propensity to cleave perpendicular to the discoidal plane. Hand pick is 42 cm long.

deposits (Allmendinger 1971; Fig. 9). These "selenite beds" are of interest in part because it has been argued for decades (e.g., Talmage and Wootton 1937) that they are the primary source of gypsum for the present-day White Sands. The presence of these large selenite crystals leads to the question of whether they grew in the bottom muds of the lake while it still contained water. Observations suggest that crystal growth may have occurred in association with shallow ground water, perhaps long after desiccation of the lake. In particular, crystal growth in the bottom muds of a lake might be expected to produce a more or less continuous stratum or shore-parallel band of interstitial crystals. The large selenite crystals along the west side of Alkali Flat, however, are present in patches ranging from hundreds of meters to as small as a few meters across, and at various stratigraphic levels. Furthermore, the selenite is commonly present within relatively loose deposits where they overlie lower-permeability beds. This association might reflect confinement and lateral movement of shallow, sulfate-enriched ground water perched above the low-permeability beds, accompanied by the displacive growth of large crystals in overlying deposits. Continuous replenishment of sulfate and calcium ions along preferred shallow flow paths may have contributed to the patchy distribution and the remarkable size achieved by some of the crystals.

Northern-margin deposits

Lithofacies

Deposits associated with Lake Otero generally contain more siliciclastic sediment and less gypsum at the northern end of the lake basin. In particular, reddish-brown muds become increasingly common to the north, as do accumulations of sand and pebbly sand in the upper part of the lake-margin sequence.

The most common lithofacies in northern-margin exposures consists of reddish-brown and pale-greenish-gray siliciclastic mud. Individual beds are generally structureless or weakly color banded to mottled and contain varying amounts of gypsum as interstitial lenticular grains. Some beds contain an abundance of fossil aquatic organisms; others do not. The red and green muds along the north side of Alkali Flat are interbedded on a scale of decimeters to meters, and in most areas are flat lying and nearly horizontally bedded. In other areas, the beds display broad (over tens to hundreds of meters), fold-like undulations with amplitudes as high as a few meters. At one place, just to the east of locality lecto in Figure 2, beds low in the section are truncated by nearly 3 m of erosion. Horizontal beds in the middle part of the section slope abruptly down to the southwest across the truncated underlying deposits, and then flatten out again over a distance of 100 m (Fig. 10).

Beds of nearly pure gypsum are present in the lower part of the lacustrine sequence in the vicinity of locality 8 along the northeast margin of the lake basin (Figs. 2, 3; Appendix D), which is probably the most basinward site examined in this study. The gypsum beds are generally fine grained (mostly silt sized), compact, structureless, ledge-forming units and include thin, dark-colored beds containing organic matter. Abundance and diversity of aquatic fossils in the gypsum at locality 8 appear to be

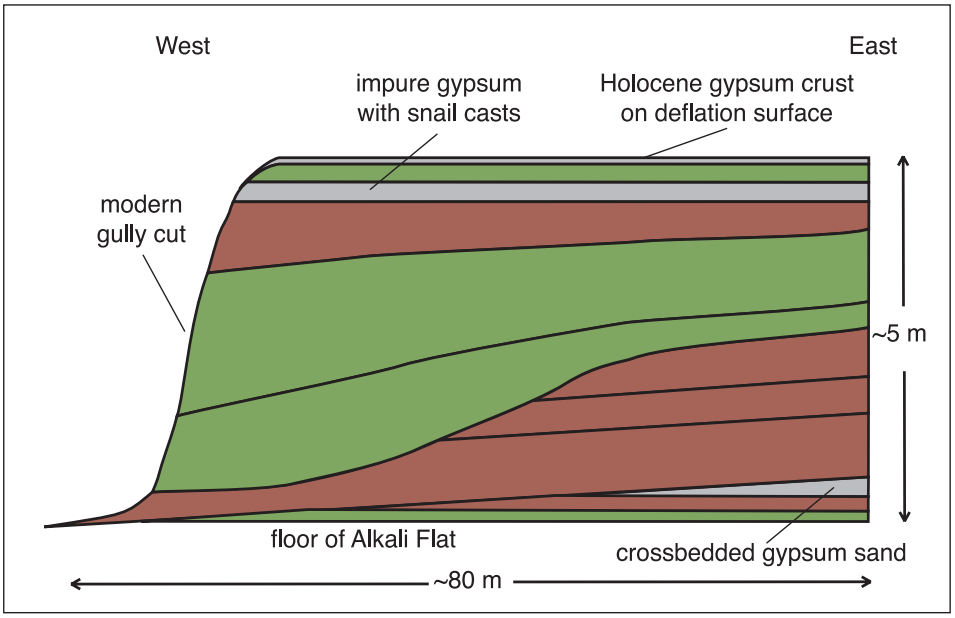

FIGURE 10—Schematic cross section of lake-margin deposits exposed along the north side of Alkali Flat, east of the stratigraphic section measured by Lucas and Hawley (2002). Deposits are predominantly reddish-brown and greenish-gray siliciclastic mud. Lower beds are truncated to the west, middle beds drape downward across the truncated beds, and upper beds are horizontal across the rest of the section. Horizontal and vertical scales are approximate, based on field sketches.

greater than in similar beds in the lower part of the lacustrine sequence along the western margin of the lake basin. The upper part of the gypsum interval at locality 8 contains indurated layers several centimeters thick that are suggestive of subaerially formed gypsum crust, and the contact with overlying deposits exhibits broad scours with at least 60 cm of vertical relief.

Siliciclastic sand and pebbly sand deposits in northern exposures are present as meandering-channel fills and as sheet-like accumulations of silty to pebbly sand. As noted by Lucas and Hawley (2002), gravels in coarse-grained deposits include igneous clasts (porphyries) derived from the northern part of the basin, including possible source terranes extending from Sierra Blanca to the Gallinas Mountains (Fig. 1). Clasts of Permian reddish-brown sandstone, derived from northern source areas, are also common.

Near Alkali Spring (Fig. 2), beds of reddish-brown and greenish-gray mud, typical of northern-margin exposures, are overlain at an elevation of ~1,204 m by variegated mud and silty to pebbly sand and gravel (Fig. 11). The color of these overlying deposits ranges through shades of red, yellow, brown, and green. Some beds exhibit cracks and root molds that have nearly destroyed color banding. Thin beds of interlaminated mud and silty fine sand are present, as are discontinuous to laterally persistent dark-gray layers enriched in organic matter. Fragments of charcoal, as large as a centimeter across, are locally abundant, and some beds contain mollusk shells.

Depositional environments of the northern margin

In the vicinity of locality 8 (Fig. 2), muds in the basal ~50 cm of the exposed sequence contain abundant lenticular gypsum silt and sand, and aquatic fossils are rare to absent. Lenses of sand and pebbly sand filling shallow channels, beds of cross-stratified transported gypsum sand, and cemented fine-grained gypsum layers are also present. The lithofacies and lack of aquatic organisms suggest that these basal beds were deposited by subaerial alluvial processes, perhaps along the margin of a gypsum-precipitating playa.

Muds overlying the basal alluvial deposits at locality 8 were probably deposited in a lake-margin environment, as indicated by fossil ostracodes and other aquatic organisms. Broad, shallow scours are present that may reflect episodes of subaerial exposure or resuspension of sediment and erosion by wave action during storms. These fossiliferous muds are overlain by approximately 2 m of compact, fine-grained gypsum as described above, with lesser interbeds of siliciclastic mud. Fish scales, ostracodes, aquatic mollusks, and plant remains are generally present in the gypsum beds. Compared with similar and probably correlative fine-grained gypsum beds along the west margin of the lake, the greater abundance and diversity of aquatic organisms in these deposits may indicate a larger and more continuous influx of ground and surface waters along the north side of the lake, and a somewhat fresher aquatic environment. The erosional surface on top of the gypsum beds at locality 8 is similar to evidence along the western margin for an extended episode of subaerial exposure before deposition of the upper part of the lacustrine sequence.

The upper part of the lacustrine sequence at locality 8 consists largely of greenish-gray

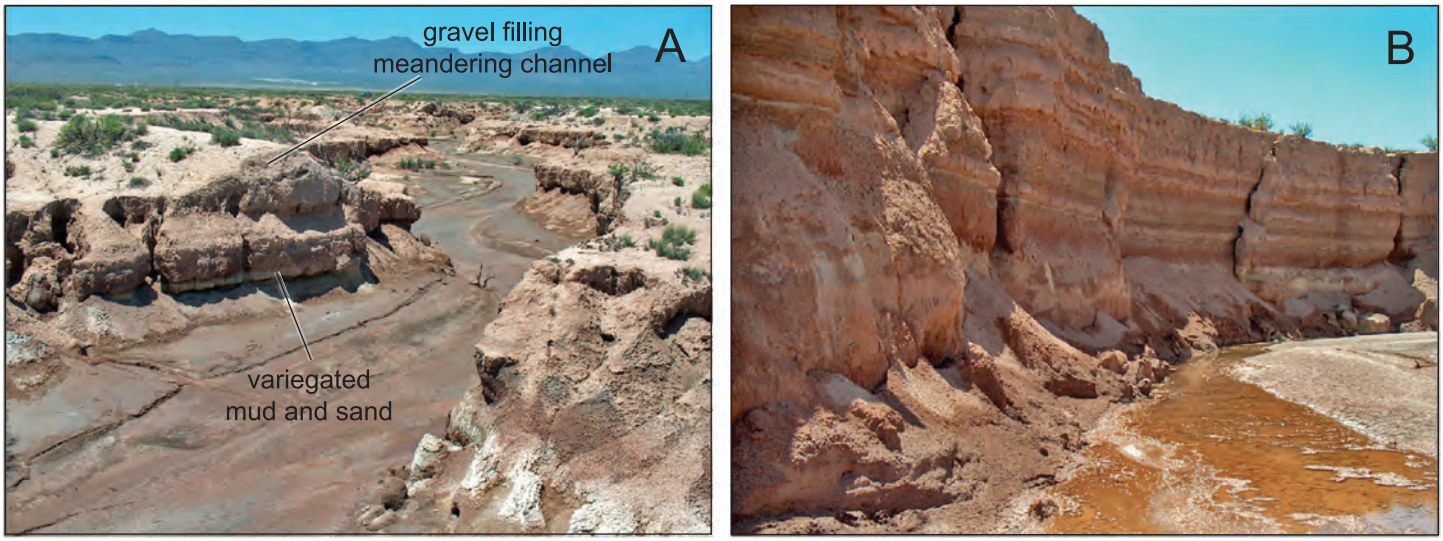

FIGURE 11—Exposures of deposits along erosional cuts near Alkali Spring. **A**—Greenish-gray, lake-margin alluvial mud along floor of drainage, overlain by fluvial-distributary mud, sand, and gravel. **B**—Closer view of variegated fluvial deposits a short distance downstream from locality shown in Figure 11A.

and reddish-brown siliciclastic muds that generally contain fossil ostracodes, plant fragments, and, in some beds, fish scales and aquatic gastropods. Stringers of fine to coarse siliciclastic sand are present in some beds. The relative increase in siliciclastic sediments in the upper part of the lake-margin sequence suggests episodes of increased fluvial discharge and basinward transport of siliciclastic sediment into the lake. The upper 3–4 m or more of the lacustrine sequence at locality 8 has been removed by deflation. This is unfortunate because the basinward position of this locality suggests that it may have accumulated a comparatively complete record of lacustrine deposition until the lake dried up.

The truncated top of the section at locality 8 is a planar, wind-deflated surface capped by a hard, ~45 cm thick crust of interlocking, lenticular selenite crystals. This surface likely represents a higher, previous level of Alkali Flat. The elevation of this surface (~1,198 m; 3,930 ft)) corresponds with the level of the erosional bench along the western margin of the lake basin, which, as discussed earlier, is capped by discontinuous deposits of tufa on that side of the lake basin.

Exposures to the north and northwest of locality 8 (e.g., localities gap and lecto in Fig. 2) consist largely of reddish-brown and pale-greenish-gray mud. The sequence at locality lecto was measured and described by Lucas and Hawley (2002) and is similar to the gap section. Both consist of a monotonous succession of red and green muds, with sand and gravelly sand more abundant toward the top. Time did not permit detailed sampling at either locality, and the stratigraphic distribution of fossils is poorly known. Aquatic gastropods are present in at least two beds at the lecto section (Gordon et al. 2002), and a sample collected from the uppermost bed of this section, immediately beneath overlying eolian deposits (unit 12 of Lucas and Hawley 2002), contains abundant, well-preserved ostracodes and calcified *Chara* oogonia in addition to aquatic gastropods, indicating a lacustrine environment. Nonetheless, it is clear that the pebbly channel sands at these localities are fluvial, and many of the siliciclastic muds in these exposures may have been deposited subaerially as well.

Deposits exposed in drainage cuts near the Alkali Spring deflation basin (Fig. 11) consist of a basal sequence of reddish-brown and greenish-gray muds, characteristic of deposits along the northern margin of Alkali Flat, and an overlying sequence of multi-colored muds and silty to gravelly sand. The depositional environment of the basal muds (with less pebbly sand) is probably some combination of marginal lacustrine and distal alluvial plain. Overlying deposits exhibit a range of lithofacies suggesting invigorated fluvial activity in the basin relative to underlying deposits. Silty sands in these overlying deposits may represent crevasse splay deposits that spread across overbank areas during flood stages. Some of the overbank deposits were churned by roots and possible shrink-swell (vertisol) processes, and dark-gray layers may represent development of organic-A soil horizons during episodes of local land-surface stability in overbank areas. Ponding in overbank areas is indicated by the presence of aquatic mollusks in some beds.

Coarse-grained beds in the upper part of the sequence contain gravel clasts as large as a few centimeters in diameter, and the sandy fills of individual meandering channels are more than 2 m thick and several meters wide, indicating an impressive amount of fluviatile transport across the low-gradient floor of the basin. Similar coarse-grained channel-fill deposits in deflation exposures to the north and east of Alkali Spring and along the cutbank of Salt Creek farther to the north indicate that deposits associated with these late Pleistocene fluvial systems extend considerable distances upstream toward headwaters in the paleowatersheds of Three Rivers, Carrizozo, and Salt Creek (Fig. 2).

Explanation(s) for the broad, fold-like undulations and truncation surfaces in the red and green muds along the northern margin of the lake basin are not obvious. Lucas and Hawley (2002) hinted that some of these bedding structures may be related to seismic activity. This is a reasonable speculation given the documented history of Pleistocene–Holocene seismic activity in the Tularosa Basin (e.g., Machette 1987; Gile 1994; Koning and Pazzaglia 2002). Other possibilities include deformation resulting from differential loading or dewatering of sediments, and syn-sedimentary processes analogous, on a small scale, to mass-movement processes in large deltas (e.g., Elliot 1986).

Lake Otero shorelines (or lack thereof)

Information regarding the elevation of Lake Otero during highstands has a bearing on a variety of issues concerning the hydrologic response of the basin to the most recent glacial climate cycle. The Seager et al. (1987) geologic map, which covers a large part of the southern Tularosa Basin, indicates a 3,950 ft (1,204 m) highstand elevation for the late Pleistocene lake. Observations made in this investigation, as discussed above, are consistent with that assessment. Nonetheless, there is an apparent perception that Pleistocene lakes in the basin covered 2,100 km^2 or more (e.g., Lucas and Hawley 2002), which corresponds to a lake elevation of approximately 1,218 m. Seager et al. (1987) allowed for the possibility of large, precursor lakes in the basin by including "lakebeds" in the description of a basin-floor map unit (Qbfg) that extends to an elevation of approximately 1,218 m.

Based on present-day topography, a 1,204-m highstand corresponds to a lake covering approximately 745 km^2 (Fig. 1). The 745 km^2 figure probably underestimates the surface area of the lake because it does not account for basin-floor areas that may have been below 1,204 m during highstands but were subsequently buried by eolian deposits associated with episodes of post-Lake Otero wind deflation. In addition, there is at least one internally drained, higher-elevation sub-basin (Tres Hermanos sub-basin in Fig. 1) that contained lakes to the east of the main body of Lake Otero (Seager et al. 1987; Allen and Love, unpublished reconnaissance 2006).

Questions regarding the extent of Lake Otero during highstands are compounded by an absence of associated, well-defined shoreline features. This lack of preserved shorelines is due largely to wind deflation and burial of downwind areas by eolian deposits (including the White Sands dune field). Siliciclastic sand, possibly derived from beach-related features along the northern lake margin, now forms dunes northeast of Alkali Flat. The west margin of the lake basin lies in proximity to the faulted front of the San Andres Mountains. Steepened gradients related to fault offsets and 10 m of wind deflation have resulted in Holocene alluvial-fan erosion, transport, and deposition, destroying or obscuring shorelines on that side of the lake. A sinuous landform on the southeast side of the lake basin, with an elevation of 1,210 m, has been identified as a shoreline of the late Pleistocene lake system by Langford (2003). The interpretation of this and similar gypsiferous landforms that are present in the southern part of the lake basin is debatable. Wind deflation of the lake floor coupled with periodic flooding and re-shaping of adjacent eolian landforms may be a more likely explanation for these features.

In short, none of the exposures examined during this investigation indicate that the late Pleistocene lake system rose to an elevation of 1,218 m. As noted above, isolated higher-elevation lakes probably existed to the east of Lake Otero in the vicinity of Tres Hermanos. The precise age, stratigraphy, and extent of these eastern lake deposits have not, to our knowledge, been investigated.

Chronology

Accelerator mass-spectrometer radiocarbon analyses of samples consisting of ostracode valves, plant fragments, and charcoal from deposits associated with Lake Otero yielded 12 radiocarbon dates ranging from 41,240 to 15,660 ^{14}C yrs B.P. (Table 1). Accuracy of these ages is subject to the usual caveats. Contamination of samples with modern carbon would cause the apparent ages to be too young. Conversely, an unknown hard water effect in aquatically derived materials could cause apparent ages to be too old (e.g., Birks 2001). Charcoal fragments were probably

TABLE 1—Radiocarbon ages from deposits associated with late Pleistocene Lake Otero.

Radiocarbon age[1]	Lab number	Material[2]	$\delta^{13}C$ 0/00[3]	Locality[4]	Depth (cm)[5]
Lake-margin deposits (Lake Otero)					
41,240 (600)	Beta 216107	ostracodes	-3.6	8	595
31,640 (350)	Beta 204417	macrophytes	-22.6	3c	210
31,500 (250)	Beta 210311	"	-22.4	3c	390
31,020 (320)	Beta 204418	"	-14.0	8	470
28,210 (260)	Beta 216108	"	-12.0	8	335
24,420 (190)	Beta 216109	charcoal	-22.7	8	245
22,800 (130)	Beta 206641	"	-23.9	AS1	480
21,720 (80)	Beta 206642	ostracodes	0.1	1d	315
21,210 (70)	Beta 216106	"	-7.6	3a	345
20,700 (70)	Beta 206643	"	-5.5	8	120
19,430 (70)	Beta 202927	macrophytes	-23.0	1d	210
15,660 (50)	Beta 216105	ostracodes	-2.3	lecto	top[6]

[1] Radiocarbon ages determined by accelerator mass spectrometry; 1-sigma error reported by the lab in parentheses.
[2] Plant materials were subjected to standard acid-base-acid pretreatment.
[3] Carbon isotopic ratios in delta notation (relative to the PDB standard); used to correct for isotopic fractionation.
[4] Localities indicated in Figure 2.
[5] Depth below top of measured section at each locality.
[6] "top" refers to the uppermost lacustrine unit at this locality (unit 12 of Lucas and Hawley 2002), which is overlain by 10+ m of post-Lake Otero eolian deposits.

transported to depositional sites by alluvial processes, and uncertainty in the duration of transport and the antiquity of the plants when they died also suggests a maximum-age interpretation for those samples. Possible reworking of previously deposited carbon in relatively high-energy, nearshore depositional environments adds additional uncertainty to the age estimates for some of the dated samples. The sample that yielded the oldest age of 41,240 ^{14}C yrs B.P. (Beta 216107) consisted of well-preserved ostracode valves, and careful preparation suggests that contamination of this sample with modern carbon was unlikely. Nonetheless, its apparent age is near the limit of the radiocarbon method and is considered to be a rough estimate of the sample's true age.

Keeping these considerations in mind, the age determinations reported here appear to provide a consistent chronology for the deposits and events associated with the late Pleistocene lake system. Basal alluvial deposits at locality 8 (Appendix D) are overlain by lacustrine muds containing fossil aquatic organisms. Taken at face value, the age of 41,240 ^{14}C yrs B.P. from locality 8 suggests that this transition from subaerial to paludal-lacustrine conditions occurred after ca. 45,000 ^{14}C yrs B.P. The fossiliferous muds from which this date was obtained have probable correlative deposits along the western margin of the lake basin. Materials suitable for radiocarbon dating have yet to be recovered from correlative western-margin deposits, however.

Overlying gypsum beds at locality 8 yielded two dates of 31,020 and 28,210 ^{14}C yrs B.P. Assuming continuous deposition of these deposits, the radiocarbon ages suggest an accumulation rate of approximately 50 cm per thousand years during gypsum precipitation. Gypsum beds in the lower part of the stratigraphic sequence along the western margin of the lake basin (locality 3c in Fig. 2; Appendix C) yielded two dates of 31,640 and 31,500 ^{14}C yrs B.P. Considering their 1-sigma analytical errors (Table 1), these ages are essentially the same. Thus, in contrast to the situation at locality 8, the radiocarbon dates from locality 3c suggest rapid sedimentation of intervening deposits. However, the lower and upper samples from locality 3c were collected from exposures separated laterally by approximately 50 m, and the upper sample was collected from a bed that was deposited in the bottom of a broad, 60-cm-deep erosional swale. This erosion raises questions about the possibility of subtle inset stratigraphic relations, or reworking and re-deposition of carbon-containing materials at this locality.

Radiocarbon ages from the upper part of the stratigraphic sequence range from 24,420 to 15,660 ^{14}C yrs B.P. The 24,420 ^{14}C yrs B.P. age from the lowest bed in the upper part of the lacustrine sequence at locality 8 probably provides the best estimate for the onset of repeated episodes of increased precipitation, enhanced surface runoff, and freshening of the lake suggested by these deposits. The date of 22,800 ^{14}C yrs B.P. from interdistributary fluvial deposits at locality AS1 (Fig. 2) is also consistent with increased fluvial activity after 24,500 ^{14}C yrs B.P. The youngest age of 15,660 ^{14}C yrs B.P. was obtained from lacustrine deposits at the top of the lecto section described by Lucas and Hawley (2002), and suggests that periods of lake expansion occurred at least until then. Bracketing ages from the upper part of the lacustrine sequence at locality 8 suggest an overall depositional rate for the lake-margin muds at that locality of 35 cm per thousand years. A depositional rate of approximately 45 cm per thousand years is indicated for the interbedded carbonate and siliciclastic muds at locality 1d along the western margin of the lake basin.

Discussion

The observations and interpretations of exposed basin-floor deposits presented above suggest that marshes and perennial lakes on the floor of Tularosa Basin were evident after about 45,000 ^{14}C yrs B.P. Information regarding older basin-floor deposits is limited, and the vertical distribution, age, and thickness of lacustrine deposits beneath the floor of Alkali Flat remains conjectural. An intriguing question is whether the floor of the basin is underlain by a vertical succession of alternating lacustrine and subaerial deposits spanning several glacial-interglacial cycles. On one hand, it is natural to presume that this would be the case given the large size of the basin and availability of transported sediment (both clastic and chemical) derived from the surrounding mountains. Topographic closure of the modern Tularosa Basin was initiated when the ancestral Rio Grande flowed eastward across Fillmore Pass (to the south of the Organ Mountains in Fig. 1), depositing a thick sequence of fluvial deposits that form the low divide on the south side of the basin. Construction of this siliciclastic sill across the southern end of the basin probably began during late Pliocene time (e.g., Seager 1981; Mack et al. 1996). Therefore, it appears that the basin has been closed long enough to have captured several glacial-interglacial cycles in its basin fill.

Much of the lacustrine sequence deposited during the most recent glacial episode has been removed from the floor of the basin by the wind. This excavation of Alkali Flat has created approximately 10 m of vertical space that may be expected to accumulate lacustrine sediments during the next glacial cycle. If that were to happen, the lacustrine sequence on the floor of the lake basin would consist largely of these future lacustrine deposits, the latest Pleistocene lakebeds having been removed by deflation during the Holocene. The obvious question is whether a similar sequence of events (glacial deposition and interglacial deflation) has occurred repeatedly in the past. If so, the stratigraphic sequence beneath the floor of Alkali Flat may not

contain the long, continuous record of successive glacial-interglacial deposits that one might expect. Downward fluctuating water tables and possible deflation may have been initiated when the Rio Grande at El Paso began to incise late in early Pleistocene time (Connell et al. 2005).

Early wetlands and shallow lakes that formed on the floor of Tularosa Basin beginning ca. 45,000 ^{14}C yrs B.P. evolved by about 30,000 ^{14}C yrs B.P. into a lake system characterized by widespread deposition of fine-grained gypsum. These gypsiferous deposits of the lower part of the lacustrine sequence contain numerous beds enriched in fragments of aquatic plants, suggesting the presence of dense stands of emergent vegetation along the shallow margins of the lake. Footprints, trackways, and skeletal elements of Pleistocene megafauna associated with the gypsiferous lake-margin deposits (Lucas et al. 2002, 2007; Morgan and Lucas 2002, 2005) suggest that these animals were attracted to the lake. It seems likely given its shallow depth, large evaporative surface area, and influx of dissolved Permian sulfate that the lake was saline and generally unsuitable for drinking. Perhaps the late Pleistocene mammals were attracted, instead, by the abundant vegetation along the margin of the lake.

The deposits associated with Lake Otero indicate a shift from chemical (sulfate) deposition to episodes of increased fluvial discharge into the lake beginning around 24,500 ^{14}C yrs B.P. Enhanced pluvial conditions after 25,000 ^{14}C yrs B.P. is consistent with chronologies for late Pleistocene lake and wetland expansions in other basins in the region. For example, the paleoclimatic reconstruction from late Pleistocene Lake Estancia (just to the north of Tularosa Basin) indicates significant increases in surface runoff and episodes of major lake expansions beginning after 24,000 ^{14}C yrs B.P. (Allen 2005). To the south, in late Pleistocene Lake King of the Salt Basin (Texas), repeated episodes of lake freshening apparently began after about 23,000 ^{14}C yrs B.P. (Wilkins and Currey 1997). Given uncertainties associated with radiocarbon chronology, the agreement in timing for the onset of significantly wetter climate, as recorded in lacustrine deposits from these neighboring basins, is good.

The record of lacustrine deposition on the floor of Tularosa Basin extends to at least 15,660 ^{14}C yrs B.P. To the north, the Lake Estancia record indicates that a major, millennium-long episode of severe drought occurred between about 15,000 and 14,000 ^{14}C yrs B.P., during which time the lake shrank to its minimum pool (Allen and Anderson 2000). This dry period was followed in Estancia Basin by two more episodes of lake expansion between ca. 14,000 and 12,500 ^{14}C yrs B.P. Additional chronology of the deposits associated with Lake Otero is needed in order to document how long lacustrine conditions persisted in the Tularosa Basin. Deposits may be present at some localities indicating episodes of lake expansion following the 15,000–14,000 ^{14}C yrs B.P. drought. However, Lake Otero may have desiccated completely during the drought, and excavation of the lake floor by wind deflation may have begun at that time. If that were the case, sediments deposited in any post-14,000 ^{14}C yrs B.P. lakes that may have existed would probably exhibit rather complicated (i.e., inset) depositional relations relative to the previously deposited lacustrine sediments. Furthermore, these younger, inset lacustrine deposits would probably be the first casualty of resumed deflation, and the potential for their preservation in the geologic record probably would be poor.

Geomorphic evidence for episodes of deflation of the relict floor of Lake Otero was discussed by Langford (2003). Langford identified three erosional scarps at progressively lower elevations around the margin of Alkali Flat. The lowest (youngest) scarp surrounds modern Lake Lucero, the next higher (Langford's L2 "shoreline") is at an elevation of approximately 1,191 m, and the highest scarp (L1) is at approximately 1,200 m. Langford speculated that deflation of the basin floor and creation of the L1 scarp occurred at the end of the Pleistocene, and that excavation to the L2 and Lake Lucero levels occurred during the mid-Holocene.

Previous work in the Estancia Basin (Allen and Anderson 2000; Anderson et al. 2002), with somewhat better chronology, documented two generations of wind deflation in that basin. The two generations of deflation were separated by an episode of wetter climate that resulted in the formation of a shallow lake between about 11,000 and 10,000 ^{14}C yrs B.P. The first generation of deflation (ca. 12,000–11,000 ^{14}C yrs B.P.) removed lacustrine sediment from the central axis of the lake floor and deposited the winnowed material to the east in a discontinuous gypsum sand sheet and in isolated mounds and ridges (probably eolian dunes originally). Expansion of the lake during the intervening episode of wetter climate reworked these deposits along the eastern shore of the lake into a series of beach ridges. The second generation of deflation began about 7,000 ^{14}C yrs B.P., and consisted of at least two episodes of extensive mid-Holocene deflation, which ultimately lowered ground water levels on the floor of the basin by approximately 10 m.

Based on the record from Estancia Basin it is probably safe to assume that most wind deflation in Tularosa Basin also occurred during the mid-Holocene. The timing of the initial episode of deflation that lowered the margin of Alkali Flat to 1,198 m is not as obvious. Perhaps excavation to the 1,198-m terrace coincided with the first-generation episode of deflation in the Estancia Basin, ca. 12,000–11,000 ^{14}C yrs B.P. Correlation of these events is consistent with evidence from both basins for a pulse of wetter climate that halted first-generation deflation. In Tularosa Basin, the evidence is in the form of tufa deposits that precipitated on the 1,198-m terrace, suggesting extensive areas of ground water seepage along the western margin and perhaps the formation of temporary lakes. In the Estancia Basin, the geomorphic evidence for a lake expansion that terminated first-generation deflation (beach ridges) is even clearer.

Alternatively, initial deflation of the floor of Lake Otero may have occurred shortly after 15,000 ^{14}C yrs B.P., at which time Lake Estancia to the north nearly desiccated. In this scenario, the tufa deposits on the 1,198-m terrace might correspond temporally with the wetter climatic conditions and renewed expansions of Lake Estancia that occurred between 14,000 and 12,500 ^{14}C yrs B.P. Cursory examination (dissolution in HCl) of a few samples of tufa from the 1,198-m terrace indicates that it contains clay minerals, probably making these samples unsuitable for uranium-series dating. In addition, insoluble residues from these samples did not contain plant fragments that might be suitable for radiocarbon dating. These preliminary observations do not rule out the possibility that samples of tufa associated with the 1,198-m terrace may be found that are amenable to radiometric dating techniques. Such data would provide additional information about the waning stages of Lake Otero and the progression of terminal Pleistocene climate changes that affected the region.

Kocurek et al. (2007) report optically stimulated luminescence (OSL) ages on core samples obtained within the crescentic dunes of White Sands National Monument, with basal clay sediment at a depth of 9 m below the land surface yielding an age of 7.3 ± 0.5 ka and gypsum sand at a depth of 6 m yielding an age of 5.2 ± 0.4 ka. Kocurek et al. (2007) suggest that the OSL ages indicate extensive deflation of Lake Otero deposits and accumulation of gypsum dunes by about 7 ka, similar in timing to the second-generation episode of deflation that occurred in the Estancia Basin to the north.

Conclusions

The development and demise of Lake Otero in the Tularosa Basin over the past ~45,000 yrs is documented using sediments preserved along the margins of the modern deflation basin of Alkali Flat. Radiocarbon ages of deposits ranging from 41,240

to 15,660 ^{14}C yrs B.P. provide information about the timing of events. Exposures low in the preserved lake sequence suggest shallow lake margins after about 45,000 ^{14}C yrs B.P. By 30,000 ^{14}C yrs B.P. Lake Otero was depositing fine-grained gypsum with abundant aquatic vegetation near shore. Aquatic vertebrate and invertebrate fauna indicate lacustrine conditions. Terrestrial megafauna trackways and lithofacies indicate shallow water and episodic subaerial exposure. Local erosional unconformities within the section show that depositional and erosional environments expanded and contracted along the lake margins, with a major episode of erosion before 25,000 ^{14}C yrs B.P. Lake Otero expanded repeatedly between ca. 24,500 and 15,500 ^{14}C yrs B.P. with evidence of increased runoff from surrounding watersheds. Maximum lake elevation during these highstands was approximately 1,204 m. Aquatic organisms thrived in the lake during highstands. The history of the demise of Lake Otero remains to be constrained using radiometric dating techniques; one could speculate that it is similar to the timing of events that occurred in the Estancia Basin just to the north, with desiccation and initial deflation between 12,000 and 11,000 ^{14}C yrs B.P., or perhaps earlier, between about 15,000 and 14,000 ^{14}C yrs B.P. Chronology of tufa deposits that are preserved along the western margin of Alkali Flat, if possible, may help to determine the timing of the initial deflation. Deflation to lower levels followed and was probably most extensive during the mid-Holocene after about 7,000 ^{14}C yrs B.P.

Acknowledgments

This study was supported by the Environmental Stewardship Division of the White Sands Missile Range (WSMR) and the New Mexico Bureau of Geology and Mineral Resources. This report has been approved for public release by WSMR for unlimited distribution; the WSMR Operational Security review was completed 31 October 2008. We thank David Bustos, Anna Szynkiewicz, and the National Park Service for facilitating access to White Sands National Monument, and Virgil Lueth for photographs of fossils. We appreciate reviews of the manuscript by Kirsten Menking, Jack Oviatt, and Fred Phillips.

References

Allen, B. D., 2005, Ice age lakes in New Mexico; *in* Lucas, S. G., Morgan, G. S., and Zeigler, K. E. (eds.), New Mexico's ice ages: New Mexico Museum of Natural History and Science, Bulletin 28, pp. 107–114.

Allen, B. D., and Anderson, R. Y., 2000, A continuous, high-resolution record of late Pleistocene climate variability from the Estancia Basin, New Mexico: Geological Society of America, Bulletin, v. 112, pp. 1444–1458.

Allen, B. D., Love, D. W., and Myers, R. G., 2006, Preliminary age of mammal footprints in Pleistocene lake-margin sediments of the Tularosa Basin, south-central New Mexico (abs.): New Mexico Geology, v. 28, no. 2, p. 61.

Allmendinger, R. J., 1971, Hydrologic control over the origin of gypsum at Lake Lucero, White Sands National Monument, New Mexico: Unpublished M.S. thesis, New Mexico Institute of Mining and Technology, Socorro, 82 pp.

Anderson, R. Y., Allen, B. D., and Menking, K. M., 2002, Geomorphic expression of abrupt climate change in southwestern North America at the glacial termination: Quaternary Research, v. 57, pp. 371–381.

Bachman, G. O., 1968, Geology of the Mockingbird Gap quadrangle, Lincoln and Socorro Counties, New Mexico: U.S. Geological Survey, Professional Paper 594-J, 43 pp.

Benson, L. V., Currey, D. R., Dorn, R. I., Lajoie, K. R., Oviatt, C. G., Robinson, S. W., Smith, G. I., and Stine, S., 1990, Chronology of expansion and contraction of four Great Basin lake systems during the past 35,000 years: Palaeogeography, Palaeoclimatology, Palaeoecology, v. 78, pp. 241–286.

Betancourt, J. L., Rylander, K. A., Penalba, C., and McVickar, J. L., 2001, Late Quaternary vegetation history of Rough Canyon, south-central New Mexico, USA: Palaeogeography, Palaeoclimatology, Palaeoecology, v. 165, pp. 71–95.

Birks, H. H., 2001, Plant macrofossils; Chapter 4 *in* Smol, J. P., Birks, H. J. B., and Last, W. M. (eds.), Tracking environmental change using lake sediments: physical and geochemical methods, v. 3: Kluwer Academic Publishers, Dordrecht, Netherlands, pp. 49–74.

Bradley, R. S., 1999, Paleoclimatology: reconstructing climates of the Quaternary: Academic Press, San Diego, 613 pp.

Broadhead, R. F., and Jones, G., 2004, Oil, natural gas, and helium potential of the Chupadera Mesa area, Lincoln and Socorro Counties, New Mexico: New Mexico Bureau of Geology and Mineral Resources, Open-file Report 478, 95 pp.

Cody, R. D., 1991, Organo-crystalline interactions in evaporite systems: the effects of crystallization inhibition: Journal of Sedimentary Petrology, v. 61, pp. 704–718.

Cody, A. M., and Cody, R. D., 1988, Gypsum nucleation and crystal morphology in analog saline terrestrial environments: Journal of Sedimentary Petrology, v. 58, pp. 247–255.

Cohen, A. S., 2003, Paleolimnology: the history and evolution of lake systems: Oxford University Press, New York, 500 pp.

Connell, S. D., Hawley, J. W., and Love, D. W., 2005, Late Cenozoic drainage development in the southeastern Basin and Range of New Mexico, southeasternmost Arizona, and western Texas; *in* Lucas, S. G., Morgan, G. S., and Zeigler, K. E. (eds.), New Mexico's ice ages: New Mexico Museum of Natural History and Science, Bulletin 28, pp.125–150.

Dreimanis, A., 1962, Quantitative gasometric determination of calcite and dolomite by using the Chittick apparatus: Journal of Sedimentary Petrology, v. 32, pp. 520–529.

Echelle, A. A., Carson, E. W., Echelle, A. F., Van den Bussche, R. A., Dowling, T. E., and Meyer, A., 2005, Historical biogeography of the New-World pupfish genus *Cyprinodon* (Teleostei: Cyprinodontidae): Copeia, v. 2005, pp. 320–339.

Elliot, T., 1986, Deltas; *in* Reading, H. G. (ed.), Sedimentary environments and facies: Blackwell Scientific Publications, Oxford, pp. 113–154.

Gile, L. H., 1994, Soils, geomorphology and multiple displacements along the Organ Mountains fault in southern New Mexico: New Mexico Bureau of Mines and Mineral Resources, Bulletin 133, 91 pp.

Gordon, M. E., Morgan, G. S., and Lucas, S. G., 2002, Fossil molluscan fauna from Pleistocene Lake Otero, Tularosa Basin, New Mexico; *in* Lueth, V., Giles, K. A., Lucas, S. G., Kues, B. S., Myers, R. G., and Ulmer-Scholle, D. (eds.), Geology of White Sands: New Mexico Geological Society, Guidebook 53, pp. 47–48.

Hawley, J. W., 1993, Geomorphic setting and late Quaternary history of pluvial-lake basins in the southern New Mexico region: New Mexico Bureau of Mines and Mineral Resources, Open-file Report 391, 28 pp.

Herrick, C. L., 1904, Lake Otero, an ancient salt lake in southeastern New Mexico: The American Geologist, v. 34, pp. 174–189.

Johnson, T. C., Scholz, C. A., Talbot, M. R., Kelts, K., Ricketts, R. D., Ngobi, G., Beuning, K., Ssemmanda, I., and McGill, J. W., 1996, Late Pleistocene desiccation of Lake Victoria and rapid evolution of cichlid fishes: Science, v. 273, pp. 1091–1093.

Kocurek, G., Carr, M., Ewing, R., Havholm, K. G., Nagar, Y. C., and Singhvi, A. K., 2007, White Sands dune field, New Mexico: age, dune dynamics and recent accumulations: Sedimentary Geology, v. 197, pp. 313–331.

Koning, D. J., and Pazzaglia, F. J., 2002, Paleoseismicity of the Alamogordo fault along the Sacramento Mountains, southern Rio Grande rift, New Mexico; *in* Lueth, V., Giles, K. A., Lucas, S. G., Kues, B. S., Myers, R. G., and Ulmer-Scholle, D. (eds.), Geology of White Sands: New Mexico Geological Society, Guidebook 53, pp. 107–119.

Kottlowski, F. E., Flower, R. H., Thompson, M. L., and Foster, R. W., 1956, Stratigraphic studies of the San Andres Mountains, New Mexico: New Mexico Bureau of Mines and Mineral Resources, Memoir 1, 132 pp.

Langford, R. P., 2003, The Holocene history of the White Sands dune field and influences on eolian deflation and playa lakes: Quaternary International, v. 104, pp. 31–39.

Lema, S. C., and Nevitt, G. A., 2004, Variation in vasotocin immunoreactivity in the brain of recently isolated populations of a Death Valley pupfish, *Cyprinodon nevadensis*: General and Comparative Endocrinology, v. 135, pp. 300–309.

Lucas, S. G., and Hawley, J. W., 2002, The Otero Formation, Pleistocene lacustrine strata in the Tularosa Basin, southern New Mexico; *in* Lueth, V., Giles, K. A., Lucas, S. G., Kues, B. S., Myers, R. G., and Ulmer-Scholle, D. (eds.), Geology of White Sands: New Mexico Geological Society, Guidebook 53, pp. 277–283.

Lucas, S. G., Morgan, G. S., Hawley, J. W., Love, D. W., and Myers, R. G., 2002, Mammal footprints from the upper Pleistocene of the Tularosa Basin, Doña Ana County, New Mexico; *in* Lueth, V., Giles, K. A., Lucas, S. G., Kues, B. S., Myers, R. G., and Ulmer-Scholle, D. (eds.), Geology of White Sands: New Mexico Geological Society, Guidebook 53, pp. 285–288.

Lucas, S. G., Allen, B. D., Morgan, G. S., Myers, R. G., Love, D. W., and Bustos, D., 2007, Mammoth footprints from the upper Pleistocene of the Tularosa Basin, Doña Ana County, New Mexico; *in* Lucas, S. G., Spielmann, J. A., and Lockley, M. G. (eds.), Cenozoic vertebrate tracks and traces: New Mexico Museum of Natural History and Science, Bulletin 42, pp. 149–154.

Machette, M. N., 1987, Preliminary assessment of paleoseismicity at White Sands Missile Range, southern New Mexico—evidence for recency of faulting, fault segmentation, and repeat intervals for major earthquakes in the region: U.S. Geological Survey, Open-file Report 87-444, 46 pp.

Mack, G. H., Seager, W. R., and Monger, H. C., 1996, Plio-Pleistocene pumice floods in the ancestral Rio Grande, southern Rio Grande rift, USA: Sedimentary Geology, v. 103, pp. 1–8.

Meinzer, O. E., and Hare, R. F., 1915, Geology and water resources of Tularosa Basin, New Mexico: U.S. Geological Survey, Water-supply Paper 343, 317 pp.

Miller, R. R., and Echelle, A. A., 1975, *Cyprinodon tularosa*, a new cyprinodontid fish from the Tularosa Basin, New Mexico: The Southwestern Naturalist, v. 19, pp. 365–377.

Morgan, G. S., and Lucas, S. G., 2002, Pleistocene vertebrates from the White Sands Missile Range, southern New Mexico; *in* Lueth, V., Giles, K. A., Lucas, S. G., Kues, B. S., Myers, R. G., and Ulmer-Scholle, D. (eds.), Geology of White Sands: New Mexico Geological Society, Guidebook 53, pp. 267–276.

Morgan, G. S., and Lucas, S. G., 2005, Pleistocene vertebrate faunas in New Mexico from alluvial, fluvial, and lacustrine deposits; *in* Lucas, S. G., Morgan, G. S., and Zeigler, K. E. (eds.), New Mexico's ice ages: New Mexico Museum of Natural History and Science, Bulletin 28, pp. 185–248.

Nelson, R. E., Klameth, L. C., and Nettleton, W. D., 1978, Determining soil gypsum content and expressing properties of gypsiferous soils: Soil Science Society of America Journal, v. 42, pp. 659–661.

Raatz, W. D., 2002, A stratigraphic history of the Tularosa Basin area, south-central New Mexico; *in* Lueth, V., Giles, K. A., Lucas, S. G., Kues, B. S., Myers, R. G., and Ulmer-Scholle, D. (eds.), Geology of White Sands: New Mexico Geological Society, Guidebook 53, pp. 141–157.

Seager, W. R., 1981, Geology of Organ Mountains and southern San Andres Mountains, New Mexico: New Mexico Bureau of Mines and Mineral Resources, Memoir 36, 97 pp.

Seager, W. R., Hawley, J. W., Kottlowski, F. E., and Kelley, S. A., 1987, Geology of the east half of Las Cruces and northeast El Paso 1° x 2° sheets, New Mexico: New Mexico Bureau of Mines and Mineral Resources, Geologic Map 57, 5 sheets, scale 1:125,000.

Seehausen, O., 2002, Patterns in fish radiation are compatible with Pleistocene desiccation of Lake Victoria and 14,600 year history for its cichlid species flock: Proceedings of the Royal Society of London (B), v. 269, pp. 491–497.

Smith, G. I., and Street-Perrott, F. A., 1983, Pluvial lakes of the western United States; *in* Porter, S. C. (ed.), Late Quaternary environments of the United States: University of Minnesota Press, Minneapolis, pp. 190–211.

Talmage, S. B., and Wootton, T. P., 1937, The nonmetallic mineral resources of New Mexico and their economic features: New Mexico Bureau of Mines and Mineral Resources, Bulletin 12, 159 pp.

Van Devender, T. R., 1990, Late Quaternary vegetation and climate of the Chihuahuan Desert, United States and Mexico; *in* Betancourt, J. L., Van Devender, T. R., and Martin, P. S. (eds.), Packrat middens—the last 40,000 years of biotic change: University of Arizona Press, Tucson, pp. 105–133.

Wilkins, D. E., and Currey, D. R., 1997, Timing and extent of late Quaternary paleolakes in the Trans-Pecos closed basin, west Texas and south-central New Mexico: Quaternary Research, v. 47, pp. 306–315.

Appendices

Description of representative exposures of lake-margin deposits associated with late Pleistocene Lake Otero. Coordinates of localities are UTM meters, Zone 13S, horizontal datum NAD 27. Cumulative thicknesses of stratigraphic units are reported in centimeters from the top downward and are rounded to the nearest 5-cm increment. Slight, strong, and violent effervescence refers to the reaction of samples with 10% HCl. Moist colors are from Munsell soil-color charts. Compositional analyses (weight-percent gypsum and carbonate) for representative sediment samples are provided in the descriptions. Gypsum is generally present as individual lenticular silt- and sand-sized grains, and as mm- to cm-sized aggregates of individual grains. Carbonate in calcareous units consists primarily of very fine (probably µm-scale) grains, but is also present as larger fragments including fossil shell material, fine-grained amorphous flakes and lumps, and as encrustations that formed on aquatic vegetation. Fossil ostracodes and mollusks were identified using published references and keys. Identifications reported here are limited to generic (rather than species) level in order to minimize identification errors, pending examination by specialists. Images of representative fossils are shown in Figure A1.

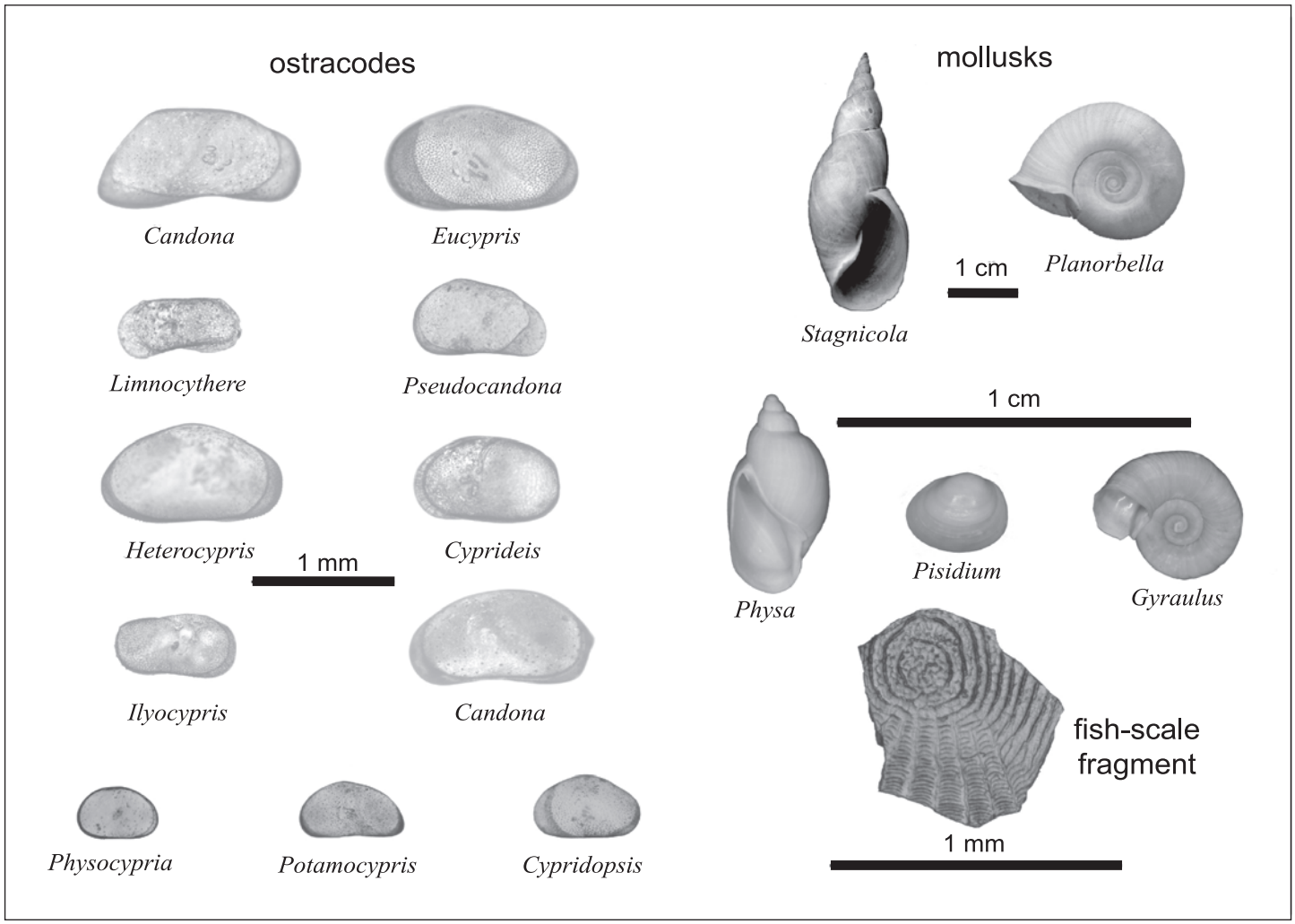

FIGURE A1—Photographs of aquatic fossils from the Tularosa Basin obtained in this study (photos courtesy of Virgil Lueth).

Appendix A

Measured section of deposits associated with late Pleistocene Lake Otero at locality 1d, upper part of lacustrine sequence. Deposits are exposed in east-facing deflation scarp along west side of Alkali Flat. Base of section is at 359086E 3641565N; top of section is at 359079E 3641560N. Ostracode genera in the sample that was sieved (from unit 3 below) include *Candona*, *Cyprideis*, *Cypridopsis*, *Cyprinotus*, *Limnocythere*, and *Potamocypris*. Aquatic pulmonate gastropod genera are represented by *Physa* and *Stagnicola*.

Unit	Description	Depth (cm)
10.	Brown gravelly piedmont alluvium (Holocene). Unit was not sampled.	0–50
9.	Light-gray gypsum crust. Unit was not sampled.	50–60
8.	White gypsum silt and sand, with interlaminated, light-gray (2.5Y 7/2) to light-olive-brown (2.5Y 5/4) calcareous clay. Slight to strong effervescence.	60–165
7.	Olive-brown to very dark-grayish-brown, thinly bedded, calcareous clay. Unit locally contains thin interbeds with abundant plant fragments, and laminae of white gypsum silt and sand. Siliciclastic sand content in some layers may be a few wt. %. Ostracodes observed on sample surfaces. Plant fragments near base of unit in correlative deposits ~50 m northwest of measured section yielded a ^{14}C age of 19,430 ± 70 (Beta 202927). Slight to strong effervescence. 2.5Y 6/2-5/4.	165–220
6.	Light-gray, calcareous, gypsiferous clay. Ostracodes observed on sample surfaces. Strong effervescence. 2.5Y 7-6/2.	220–270
5.	White, calcareous gypsum silt and sand. Ostracodes observed on sample surfaces. Strong effervescence. 10YR 8/1.	270–290
4.	Light-olive-gray/brownish-yellow (mottled), calcareous clay. Strong to violent effervescence. 5Y 5-6/2 with 10YR 6/6 mottling.	290–310
3.	Light-gray carbonate mud. Sieve residues contain calcareous casts and molds of vegetation, ostracodes, gastropods, and fish scales. Ostracode valves yielded a ^{14}C age of 21,720 ± 80 (Beta 206642). Violent effervescence. 10YR 7/2.	310–320
2.	Light-olive-gray/brownish-yellow (mottled), calcareous clay. Strong to violent effervescence. 5Y 5-6/2 with 10YR 6/6 mottling.	320–420
1.	Light-gray carbonate mud. Contains scattered lenticular gypsum grains. Ostracodes and fragments of gastropod shells observed on sample surfaces. Violent effervescence. 10YR 7/2.	420–440
Base of exposed section.		

Appendix B

Measured section of deposits associated with late Pleistocene Lake Otero at locality 3a, upper part of lacustrine sequence. Deposits are exposed in east-facing deflation scarp along west side of Alkali Flat. Base of section is at 358223E 3644612N; top of section is at 358203E 3644608N. Ostracode genera in the locality 3a section include *Candona*, *Cyprideis*, *Cypridopsis*, *Cyprinotus*, *Darwinula*, *Dolerocypris*, *Limnocythere*, and *Potamocypris*. Aquatic pulmonate gastropod genera include *Gyraulus*, *Physa*, and *Stagnicola*.

Unit	Description	Depth (cm)
15.	Pale-brown tufa. Contains abundant, mm-scale voids, some of which are lined with white carbonate. Elongate voids are present that appear to be casts of plant stems. Violent effervescence. 10YR 6-7/3.	0–15
Interval from 15 to 210 cm is poorly exposed, with a thick cover of colluvium. Samples in this interval were collected using a bucket auger.		
14.	Pinkish-white, gypsiferous, calcareous silt and clay. Sample was not sieved. Violent effervescence. 5YR 8/3 to 7.5YR 8/2.	15–45
13.	White, calcareous gypsum silt and sand, with thin, light-olive-gray (5Y 6/2) interbeds of gypsiferous, calcareous clay (gypsum: 15%, carbonate: 19% in one of the clay layers). Also contains thin stringers of hard, white carbonate mud (gypsum: 4%, carbonate: 88%). No fossils evident. Slight to violent effervescence.	45–110
12.	White gypsum silt and sand, with light-gray layers enriched in calcareous clay. Probably similar to unit 11 below, but lamination structure was disturbed during augering. No fossils evident. Slight to violent effervescence. Gypsum content in four subsamples from this interval ranges from 64 to 85%, carbonate 2 to 23%.	110–210
11.	White gypsum silt and sand, with interlaminated, light-gray (2.5Y 7/2) to light-olive-gray (5Y 6/2) calcareous clay. No fossils evident. Slight to violent effervescence. Gypsum: 81%, carbonate: 8%.	210–220
10.	White gypsum silt and sand, with interlaminated, light-gray calcareous clay. Similar to unit 11 above, but with a somewhat higher clay content. Gypsum: 60%, carbonate: 17%.	220–260
9.	White gypsum silt and sand, with interlaminated, light-gray clay. Similar to unit 11 above. Sample was not sieved. Gypsum: 91%, carbonate: 1%.	260–280
8.	Light-gray, calcareous, gypsiferous clay. Lower 5 cm of unit exhibits white and pale-yellow (2.5Y 7/4) color banding. Undispersed clay pellets in sieve residues include tubular plant casts stained with Fe-Mn oxides. Ostracodes are present but rare. Strong to violent effervescence. 2.5Y 7/2. Gypsum: 34%, carbonate: 28%.	280–295
7.	Light-olive-gray/brownish-yellow (mottled), calcareous clay. Sieve residues contain calcareous and siliceous casts and molds of vegetation, shell material (ostracodes, gastropods, foraminifera), and fish scales and skeletal elements. Violent effervescence. 5Y 6/2 with 10YR 6/6 mottling.	295–330
6.	Light-gray carbonate mud. Sieve residues contain calcareous casts and molds of vegetation, ostracodes, gastropods, and fish scales. Ostracode valves yielded a ^{14}C age of 21,210 ± 70 (Beta 216106). Violent effervescence. 10YR 7/2. Gypsum: 1%, carbonate: 63%.	330–355
5.	Light-olive-gray/brownish-yellow (mottled), calcareous clay. Sieve residues contain calcareous and siliceous casts and molds of vegetation, shell material (ostracodes, gastropods), and fish scales and skeletal elements. Violent effervescence. 5Y 6/2 with 10YR 6/6 mottling. Gypsum: 4%, carbonate: 25%.	355–395

4.	Light-gray carbonate mud. Similar to unit 6 above. Violent effervescence. 10YR 7/2. Gypsum: 2%, carbonate: 64%.	395–405
3.	Light-olive-gray/brownish-yellow (mottled), calcareous clay. Similar to unit 5 above, except that calcareous casts and molds of vegetation are rare. Violent effervescence. 5Y 6/2 with 10YR 6/6 mottling. Gypsum: 3%, carbonate: 37%.	405–435
2.	White carbonate mud. Contains ostracodes and calcareous casts and molds of vegetation. Violent effervescence. 10YR 8/2. Gypsum: <1%, carbonate: 81%.	435–490
1.	Light-olive-gray clay and carbonate mud. Contains ostracodes, gastropods, skeletal elements of fish, and calcareous casts and molds of vegetation. Strong effervescence. 5Y 6/2. Gypsum: 2%, carbonate: 46%.	490–515

Base of exposed section.

Appendix C

Measured section of deposits associated with late Pleistocene Lake Otero at locality 3c, lower part of lacustrine sequence. Deposits are exposed in south-facing deflation scarp and in drainage cuts along west side of Alkali Flat. Base of section is at 358492E 3645460N; top of section is at 358493E 3645487N. Ostracode genera in the locality 3c section include *Candona*, *Cyprideis*, *Cypridopsis*, *Cyprinotus*, and *Limnocythere*. Gastropod shells in the samples that were sieved are fragmented and include conispiral and planispiral forms as well as toothed aperture fragments of *Planorbula* (?).

Unit	Description	Depth (cm)
10.	Brown gypsum sand and silt, with calcareous sand, silt, and clay (Holocene). Lower ~40 cm is brown (10YR 5/3), overlying deposits are pale brown (10YR 7/3). Top of unit is capped by a weak gypsum crust. Sample was not sieved. Violent effervescence. Lower brown deposits contain a higher content of siliciclastics and may have been deposited as alluvium, overlying deposits by eolian processes (?).	0–160
9.	White carbonate mud, with siliciclastic clay and gypsum. Sample was not sieved. Violent effervescence. 2.5Y 8/2. Gypsum: 11%, carbonate: 59%.	160–165
8.	White, calcareous, fine-grained gypsum. Gypsum is present primarily as silt-sized grains. Sample was not sieved. Strong effervescence.	165–190
7.	Light-gray, calcareous, gypsiferous clay. Sieve residues consist primarily of undispersed lumps of calcareous clay with intergrowths of lenticular gypsum silt and sand; gypsum sand grains and aggregates are also present. No aquatic fossils evident except for rare plant fragments. Strong effervescence. 2.5Y 7/2.	190–205
6.	Dark-gray to black calcareous clay. 10 cm thick along line of measured section, unit thickens somewhat to the west where it descends into a ~60-cm-deep swale. Unit locally contains an abundance of plant fragments. Plant fragments from a sample collected near the bottom of the swale to the west of the measured section yielded a ^{14}C age of 31,640 ± 350 (Beta 204417). Contains ostracodes, gastropods, and calcareous encrustations on plants, including *Chara* oogonia. Violent effervescence.	205–215
5.	Gypsum silt and sand in a light-brownish-gray clay matrix. Similar to unit 7 above, except for color and a higher content of sand-sized gypsum grains and aggregates. No fossils evident. Strong effervescence. 2.5Y 6/2. Gypsum: 55%.	215–265
4.	White, compact, fine-grained gypsum. Individual gypsum grains are primarily silt sized, but sand-sized lenticular grains are common. Unit contains two beds of dark-gray calcareous clay enriched in organic matter, at top and 35 cm below top of unit. Sieve residues from organic clay layers contain calcareous casts and molds of vegetation, ostracodes, and aquatic gastropods. Slight to violent effervescence. Gypsum: 82% (gypsum bed at 280–300 cm).	265–315
3.	Gypsum silt and sand in a light-brownish-gray clay matrix. Similar to unit 5 above. Strong effervescence. 2.5Y 6/2. Gypsum: 57%.	315–395
2.	White, compact, fine-grained gypsum. Similar to unit 4 above. Unit contains two thin beds of dark-gray calcareous clay. Plant fragments from a sample collected in what appear to be correlative deposits ~40 m west-southwest of measured section yielded a ^{14}C age of 31,500 ± 250 (Beta 210311). Slight to violent effervescence.	395–405
1.	Gypsum silt and sand in a light-brownish-gray clay matrix. No fossils evident. Strong effervescence. 2.5Y 6/2. Gypsum: 70%.	405–485

Base of exposed section. Exposures in shallow drainage cuts to the east of measured section suggest that the deposits at locality 3c are underlain by thinly interbedded to interlaminated gypsum sand and siliciclastic clay.

Appendix D

Measured section of deposits associated with late Pleistocene Lake Otero at locality 8, lower and upper part of lacustrine sequence. Deposits are exposed in south-facing deflation scarp along northeast side of Alkali Flat. Base of section is at 365683E 3653157N; top of section is at 365635E 3653226N. Post-Lake Otero wind deflation removed at least 3 m of the upper part of the lacustrine sequence at this locality. A schematic profile of the section showing the distribution of radiocarbon dates is illustrated in Figure A2. Ostracode genera in the locality 8 deposits include *Candona*, *Chlamydotheca*, *Cyprideis*, *Cypridopsis*, *Cyprinotus*, *Darwinula*, *Eucypris*, *Ilyocypris*, *Limnocythere*, *Physocypria*, *Potamocypris*, and *Pseudocandona*. Aquatic pulmonate gastropod genera include *Gyraulus*, *Physa*, *Planorbella*, and *Stagnicola*. Pelecypods are represented by *Pisidium*.

Unit	Description	Depth (cm)
27.	Large gypsum crystals (selenite) in a matrix of light-olive-brown to dark-grayish-brown calcareous clay. Selenite consists of yellowish-brown, translucent to opaque, cm-scale, interlocking lenticular crystals. Clay matrix is strongly effervescent. Sample was not sieved. 2.5Y 5/6 to 2.5Y 4/2.	0–45
26.	Reddish-brown, gypsiferous, calcareous clay. Contains ostracodes. Strong effervescence. 5YR 4/3. Gypsum: 12%, carbonate: 19%.	45–70
25.	Olive-gray gypsiferous clay. Contains fish scales and unidentified vertebrate skeletal elements. Slight effervescence. 5Y 5/2.	70–90
24.	Reddish-brown, calcareous, gypsiferous clay. Contains ostracodes and aquatic gastropods. Strong effervescence. 5YR 4/3.	90–115
23.	Olive, gypsiferous, calcareous clay. Large, well-preserved gastropod shells are very abundant in this unit; also contains ostracodes and fish scales. Ostracode valves yielded a ^{14}C age of 20,700 ± 70 (Beta 206643). Strong effervescence. 5Y 5/3 with 5YR 5/6 mottling.	115–125

22.	Yellowish-red gypsiferous clay at base, grading up to dark-gray clay at top. Sieve residues contain irregularly shaped lumps of rust-colored Fe-Mn oxides, some of which appear to bear impressions of plant fragments. Aside from these possible plant-fragment traces, no fossils are evident. Slight effervescence. 5YR 4/6 (base) and 7.5YR 4/0 (top).	125–135
21.	Olive, sandy, calcareous clay, with interlaminated white gypsum silt and sand. Similar to unit 19 below, but contains thin stringers of siliciclastic sand and exhibits brownish-yellow Fe-Mn oxide mottling. Strong effervescence. 5Y 5/3 with 10YR 6/6 mottling. Gypsum: 23%, carbonate: 24%.	135–175
20.	Reddish-brown, calcareous, gypsiferous, sandy clay. Contains ostracodes and approximately 10–20% sand with scattered granules. Violent effervescence. 5YR 5/3.	175–185
19.	Olive, sandy, calcareous clay, with interlaminated white gypsum silt and sand. Unit contains a gypsum layer at the base that thickens locally to ~10 cm. Includes minor sand with scattered granules. Contains ostracodes. Strong effervescence. 5Y 5/2.	185–240
18.	Olive and weak-red calcareous clay. Unit is 10 cm thick along line of measured section, thickens laterally to the west where it contains stringers of sand and truncates underlying gypsum. Contains ostracodes, vertebrate skeletal remains, and fish scales. Fragments of charcoal yielded a ^{14}C age of 24,420 ± 190 (Beta 216109). Strong effervescence. 5Y 5/3 and 2.5YR 4/2. Gypsum: 4%, carbonate: 23%.	240–250
17.	Light-gray to white, fine-grained gypsum silt and sand. Lower 60 cm is similar to unit 15 below and contains one thin bed enriched in organic matter 30 cm above base of unit. Upper 55 cm contains two ~10-cm-thick, indurated beds separated by comparatively loose gypsum silt and sand. Contains ostracodes and gastropods. Plant fragments from the dark layer 30 cm above base of unit yielded a ^{14}C age of 28,210 ± 260 (Beta 216108). 10YR 7/2 (base), white (top).	250–365
16.	Light-gray, calcareous, gypsiferous clay. Contains ostracodes. Violent effervescence. 2.5Y 7/2.	365–380
15.	Light-gray, compact, fine-grained gypsum. Individual gypsum grains are primarily silt sized, with lesser sand-sized grains and granular aggregates. General appearance in outcrop is structureless, but subtle color variations on bedding planes reveal sub-centimeter-scale vermiform structures that may represent infilled burrows or rhizome traces. Unit contains thin (up to several cm thick) gray to dark-gray beds enriched in organic matter at 25, 35, 55, and 85 cm below top of unit. The dark layer 55 cm below the top contains some light-gray clay. These dark layers are discontinuous locally, but appear to persist laterally on the scale of the outcrop (hundreds of meters). Sieve residues consist largely of undispersed lumps of gypsum silt, and contain calcareous casts and molds of vegetation, fossil shells (ostracodes, gastropods, pelecypods), and vertebrate skeletal elements and fish scales. Plant fragments from the dark layer at the base of the unit yielded a ^{14}C age of 31,020 ± 320 (Beta 204418). Slight to strong effervescence. 10YR 7/2.	380–470
14.	Pale-olive and light-reddish-brown, sandy, calcareous, gypsiferous clay. Olive colored and 25 cm thick along line of measured section. Unit thickens to the west, cutting out the underlying gypsum bed. Basal sediments in the scour and fill to the west are light reddish brown and contain stringers of sand with minor granules. Contains ostracodes, gastropods, and fish scales. Violent effervescence. 5Y 6/3 and 5YR 6/3.	470–495
13.	Light-gray, compact, fine-grained gypsum. Similar to unit 15 above. A thin, dark layer enriched in organic matter is present at the top of the unit. Slight effervescence. Sample was not sieved. 10YR 7/2. Gypsum: 85%, carbonate: 2%.	495–520
12.	Light-brownish-gray, calcareous, gypsiferous clay. Contains ostracodes and gastropods. Violent effervescence. 2.5Y 6/2.	520–555
11.	Reddish-gray, sandy, calcareous, gypsiferous clay. Includes minor (a few %) sand and rare granules. Contains ostracodes. Violent effervescence. 5YR 5/2.	555–580
10.	Olive, calcareous, gypsiferous clay. Unit contains relatively large (up to ~1 cm wide), subspherical to vermiform segregations of white gypsum silt to very fine sand, giving the unit a mottled green and white appearance. Contains ostracodes and unidentified vertebrate skeletal elements. Ostracode valves yielded a ^{14}C age of 41,240 ± 600 (Beta 216107). Violent effervescence. 5Y 5/3. Gypsum: 28%, carbonate: 22%.	580–605
9.	Light-gray, calcareous, gypsiferous clay. Sieve residues contain rare ostracode valves and calcareous casts and molds of vegetation. Strong effervescence. 2.5Y 7/2.	605–645
8.	Light-brown, calcareous, gypsiferous clay. Similar to unit 9 above except for color. 7.5YR 6/4.	645–655
7.	Gypsum silt and sand in a light-gray clay matrix. No fossils evident. Slight effervescence. 10YR 7/2. Gypsum: 73%, carbonate: 4%.	655–675
6.	Gypsum silt and sand in a light-reddish-brown clay matrix. Similar to unit 7 above except for color. 5YR 6/3.	675–690
5.	Light-brown, silty gypsum sand. Individual gypsum grains are primarily lenticular, very fine to medium sand. Larger gypsum grains (up to coarse sand) are broken and abraded. No fossils evident. Gypsum sand deposits at a similar stratigraphic position in better exposures to the east are cross-stratified. Slight effervescence. 7.5YR 6/4.	690–705
Base of exposed section. Units described below were sampled using a bucket auger.		
5. (cont.)	Light-brown, silty gypsum sand.	705–730
4.	Gypsum silt and sand. Upper 40 cm is white, relatively pure gypsum (gypsum: 83%, carbonate: 5%), and the upper 10 cm is a hard, indurated crust. Underlying deposits are somewhat less pure (gypsum: 63%, carbonate: 17%) and contain a few thin beds enriched in calcareous clay. No fossils evident. Slight to strong effervescence.	730–795
3.	Light-yellowish-brown, gypsiferous, silty sand. Sand is predominantly fine to medium grained, with lesser coarse sand and scattered granules. Gypsum is present primarily as sand-sized lenticular grains and as aggregates of smaller grains. No fossils evident. Slight effervescence. 2.5Y 6/4 to 10YR 6/4.	795–815
2.	Reddish-brown, calcareous, gypsiferous mud. No fossils evident. Strong effervescence. 5YR 5/3.	815–825
1.	White gypsum silt and sand. Unit is indurated. Sample was not sieved. Slight effervescence.	825–835
Base of sampled section.		

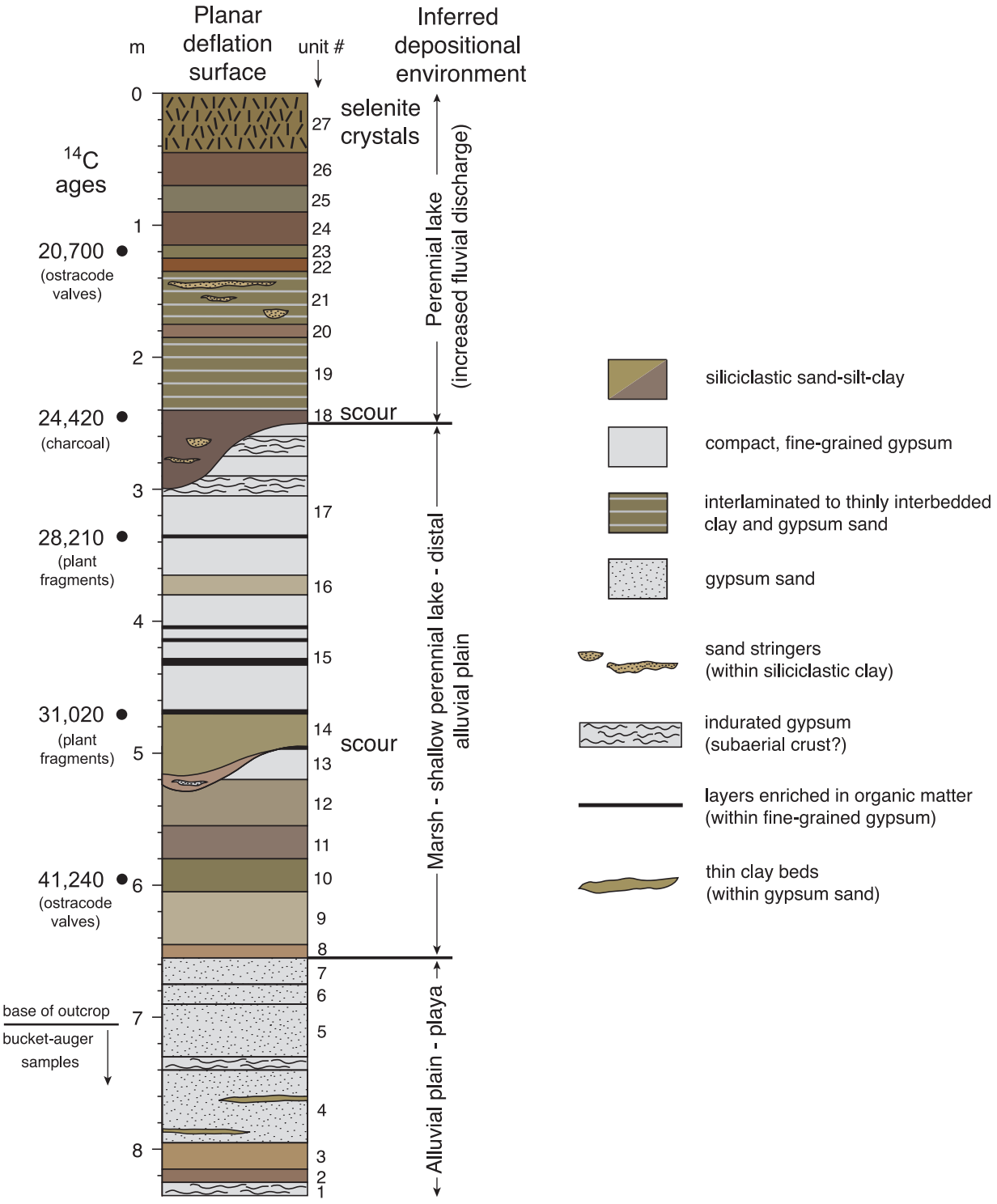

FIGURE A2—Measured section showing radiocarbon ages and inferred depositional environments at locality 8, northeast margin of Alkali Flat.

For additional metric to English conversion, use the following:

To convert	Divide by
centimeters to inches	2.540
meters to feet	0.3048
kilometers to miles	1.609
square kilometers to square miles	2.590